

Light-Activated Olefin Metathesis: Catalyst Development, Synthesis, and Applications

Or Eivgi,[§] Ravindra S. Phatake,[§] Noy B. Nechmad,[§] and N. Gabriel Lemcoff*



Cite This: *Acc. Chem. Res.* 2020, 53, 2456–2471



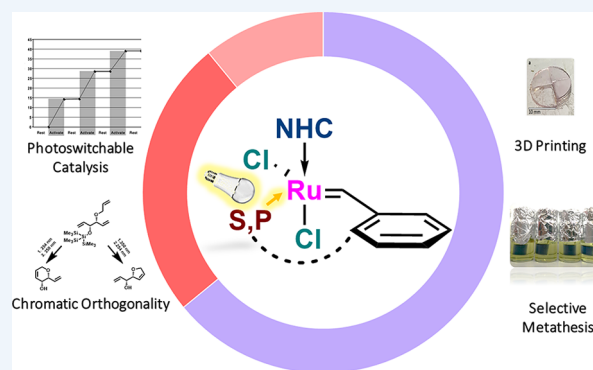
Read Online

ACCESS |

Metrics & More

Article Recommendations

CONSPECTUS: The most important means for tuning and improving a catalyst's properties is the delicate exchange of the ligand shell around the central metal atom. Perhaps for no other organometallic-catalyzed reaction is this statement more valid than for ruthenium-based olefin metathesis. Indeed, even the simple exchange of an oxygen atom for a sulfur atom in a chelated ruthenium benzylidene about a decade ago resulted in the development of extremely stable, photoactive catalysts. This Account presents our perspective on the development of dormant olefin metathesis catalysts that can be activated by external stimuli and, more specifically, the use of light as an attractive inducing agent. The insight gained from a deeper understanding of the properties of *cis*-dichlororuthenium benzylidenes opened the doorway for the systematic development of new and efficient light-activated olefin metathesis catalysts and catalytic chromatic-orthogonal synthetic schemes. Following this, ways to disrupt the ligand-to-metal bond to accelerate the isomerization process that produced the active precatalyst were actively pursued. Thus, we summarize herein the original thermal activation experiments and how they brought about the discoveries of photoactivation in the sulfur-chelated benzylidene family of catalysts. The specific wavelengths of light that were used to dissociate the sulfur–ruthenium bond allowed us to develop noncommutative catalytic chromatic-orthogonal processes and to combine other photochemical reactions with photoinduced olefin metathesis, including using external light-absorbing molecules as “sunscreens” to achieve novel selectivities. Alteration of the ligand sphere, including modifications of the N-heterocyclic carbene (NHC) ligand and the introduction of cyclic alkyl amino carbene (CAAC) ligands, produced more efficient light-induced activity and special chemical selectivity. The use of electron-rich sulfoxides and, more prominently, phosphites as the agents that induce latency widened the spectrum of light-induced olefin metathesis reactions even further by expanding the colors of light that may now be used to activate the catalysts, which can be used in applications such as stereolithography and 3D printing of tough metathesis-derived polymers.



KEY REFERENCES

- Ben-Asuly, A.; Aharoni, A.; Diesendruck, C. E.; Vidavsky, Y.; Goldberg, I.; Straub, B. F.; Lemcoff, N. G. Photoactivation of Ruthenium Olefin Metathesis Initiators. *Organometallics* 2009, 28, 4652–4655.¹ This work discloses the first photoactive sulfur-chelated olefin metathesis catalysts.
- Levin, E.; Mavila, S.; Eivgi, O.; Tzur, E.; Lemcoff, N. G. Regioselective Chromatic Orthogonality with Light Activated Metathesis Catalysts. *Angew. Chem., Int. Ed.* 2015, 54, 12384–12388.² A concept work on guiding a metathesis-based reaction sequence outcome using light only.
- Eivgi, O.; Guidone, S.; Frenklah, A.; Kozuch, S.; Goldberg, I.; Lemcoff, N. G. Photoactivation of Ruthenium Phosphite Complexes for Olefin Metathesis. *ACS Catal.* 2018, 8, 6413–6418.³ Discovery of the photoactivation feature of the commercially available ruthenium phosphite complex *cis*-Caz-1, making photoinduced olefin metathesis widely accessible.

- Eivgi, O.; Vaisman, A.; Nechmad, N. B.; Baranov, M.; Lemcoff, N. G. Latent Ruthenium Benzylidene Phosphite Complexes for Visible Light Induced Olefin Metathesis. *ACS Catal.* 2020, 10, 2033–2038.⁴ A new generation of photoactive phosphite complexes for visible-light-induced metathesis and 3D printing applications.

INTRODUCTION

Since the emergence of well-defined transition metal catalysts, olefin metathesis has evolved to become a handy paintbrush for molecular artists in industry and academia.⁵ With a plethora of

Received: August 5, 2020

Published: September 29, 2020



Scheme 1. Evolution of Light-Induced Olefin Metathesis Catalysts and Applications by the Lemcoff Research Group (Year of Publication in Parentheses)

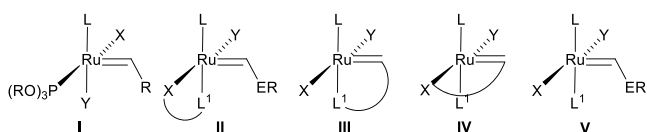
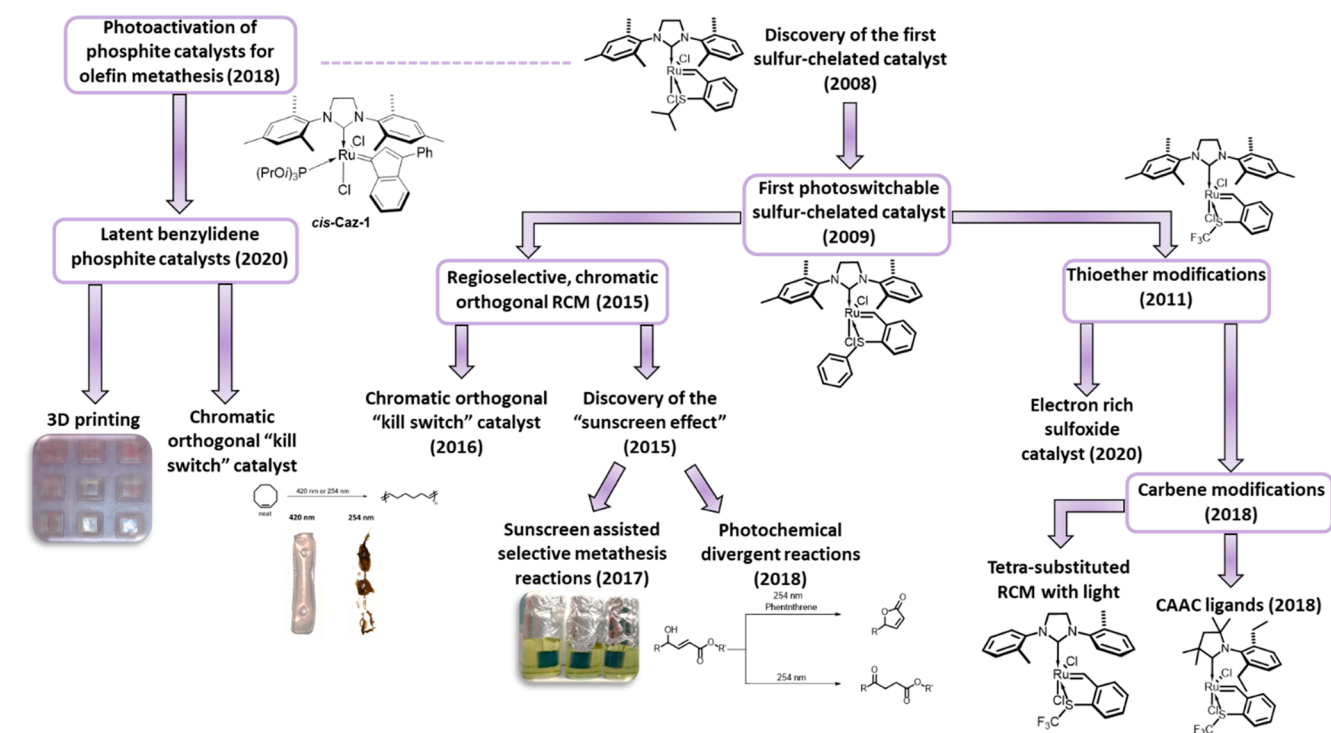


Figure 1. Models of latent ruthenium olefin metathesis catalysts. L = PCy₃, NHC, CAAC; L¹ = electron-donating group (P, N, O, S); E = O, NR, S; X, Y = anionic ligand.

options to form and reshape carbon–carbon double bonds, olefin metathesis is the method of choice for the synthesis of macrocycles⁶ and heavy-duty polymeric materials⁷ and even for the preparation of simple commodity chemicals from oil waste products and biomass.⁸ The flexible framework of ruthenium-based

complexes has opened up many research avenues for the development of task-specific catalysts,⁹ such as catalysts embedded with asymmetric ligands for enantioselective olefin metathesis reactions,¹⁰ catalysts that specialize in ring-closing metathesis (RCM) of macrocyclic structures,¹¹ catalysts for Z-selective¹² and stereoretentive¹³ olefin metathesis reactions, and fast-initiating catalysts for ring-opening metathesis polymerization (ROMP).¹⁴ Slow-initiating or latent metathesis catalysts are an important class of initiators that require the application of an external stimulus (heat, light, mechanical force, etc.) in order to promote metathesis reactions.¹⁵ Particularly attractive is the use of light,¹⁶ allowing stereolithographic 3D printing¹⁷ and the development of chromatic-orthogonal processes.¹⁸ The evolution

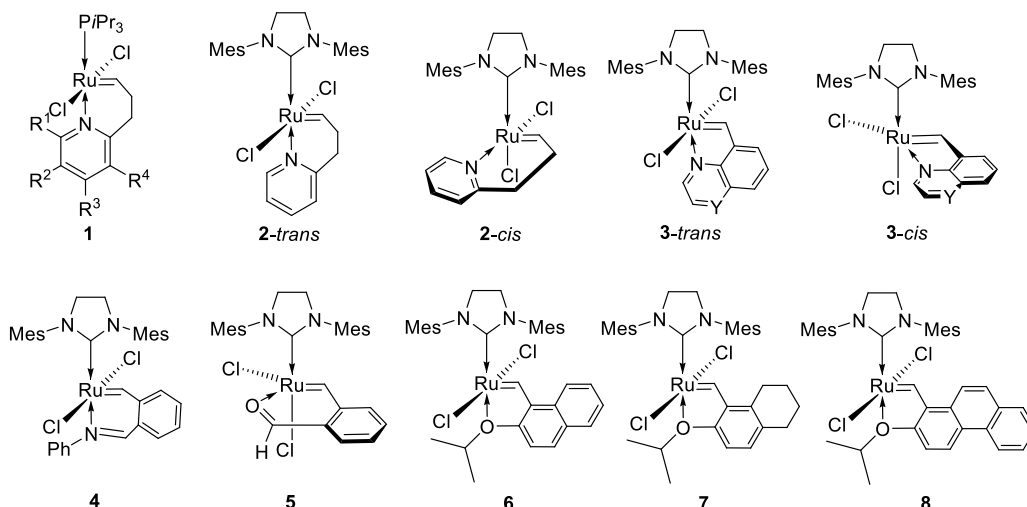


Figure 2. Selected latent ruthenium metathesis catalysts bearing chelating alkylidene ligands.

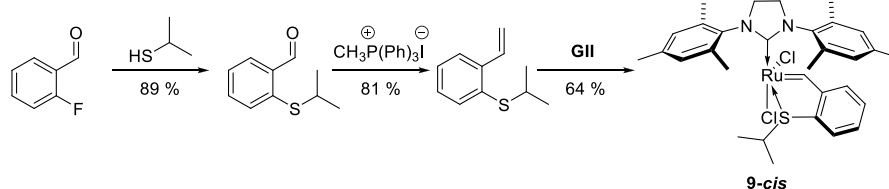
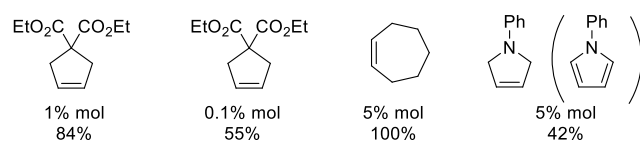
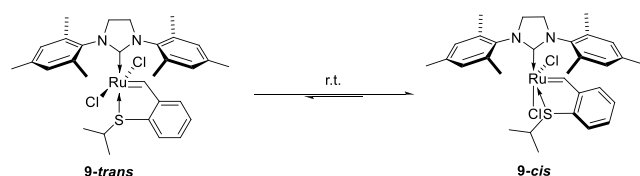
Scheme 2. Synthesis of the First Sulfur-Chelated Ruthenium Benzylidene Complex, **9-cis**Scheme 3. Thermal Equilibrium between **9-trans** and **9-cis**

Figure 3. RCM reaction products obtained using catalyst **9-cis**. Reaction conditions: 0.1 M substrate in toluene, 90 °C, 2 days. Conversions were measured using GC–MS and ^1H NMR spectroscopy.

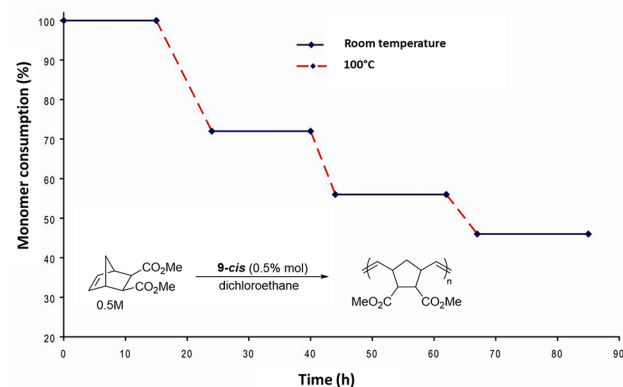


Figure 4. Thermoswitchable behavior of **9-cis**: 0.5 M dimethyl 5-norbornene-2,3-dicarboxylate in 1,2-dichloroethane with 0.5 mol % **9-cis** in a sealed vessel. Monomer consumption was measured by GC–MS.

of light-induced olefin metathesis from our group's perspective will be unfolded in this Account, and its historic flow is briefly depicted as a roadmap in Scheme 1.

STRATEGIES IN THE DESIGN OF LATENT CATALYSTS

The “magic bullet” of a latent metathesis catalyst would be a catalyst that remains inactive even when mixed with the most reactive of substrates but is able to efficiently catalyze the desired reaction when it is turned on in response to a specific external stimulus. Over the years a few approaches to slow down the initiation of olefin metathesis precatalysts have been introduced, and several latent catalysts have been reported.^{15a,19} The main tactic usually perused is strengthening a metal–ligand bond to lower the initiation rate.²⁰ In many cases, this is accomplished by forming a bidentate chelate, which hinders dissociation. Figure 1

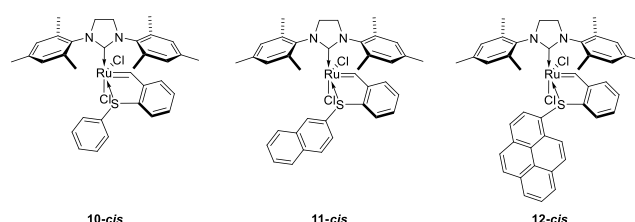


Figure 5. Sulfur-chelated olefin metathesis catalysts with aromatic groups on the thioether.

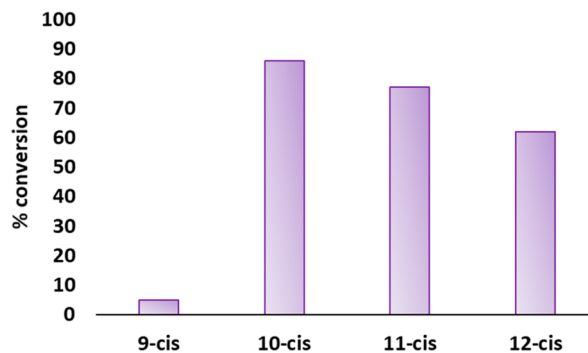
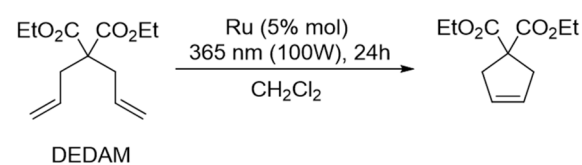
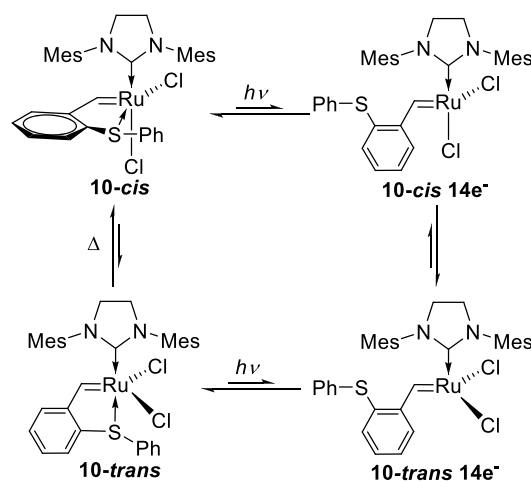


Figure 6. UV-induced RCM of DEDAM using catalysts **9-cis**, **10-cis**, **11-cis**, and **12-cis**.

Scheme 4. Proposed Photoisomerization Mechanism



presents a summary of the prevailing strategies followed for the creation of latent ruthenium-based initiators.

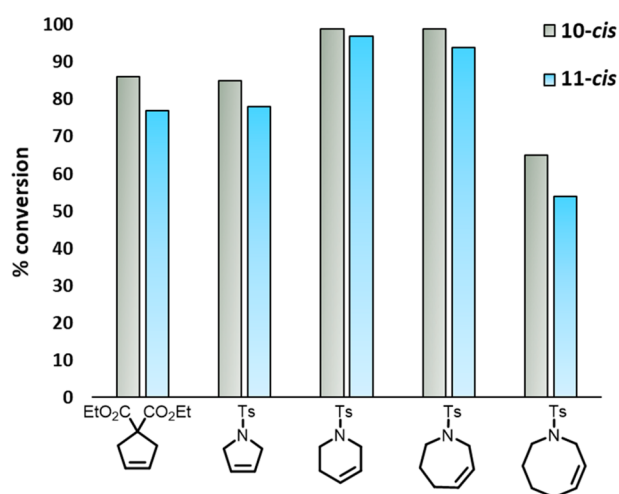


Figure 7. Photoinduced RCM with **10-cis** and **11-cis**. Reaction conditions: 5 mol % catalyst and 0.1 M substrate in CH_2Cl_2 ; UV irradiation at 365 nm for 5 h. Conversions were determined by GC–MS.

Type I latent systems (Cazin catalysts)²¹ combine a phosphite ($\text{P}(\text{OR})_3$) and a strongly σ -electron-donating ligand that are more stable in a *cis* geometry with respect to one another. This ligand configuration is inactive for olefin metathesis, and ligand dissociation is necessary for activation. In type II systems, a donor ligand is tethered to one of the anionic ligands. In this case the chelation decelerates both initiation and propagation,²² and therefore, this layout is optimally used in acid-switchable systems.²³ In the case of type III systems, a chelating carbene ligand is used. This is the most common type of ligand chelation. Here, decoordination of L^1 is entropically disfavored, and consequently, the initiation is slowed down.²⁴ Finally, type IV systems display chelation via the alkylidene and anionic ligands.²⁵ Another prominent strategy to impose latency is to substitute the carbene moiety with an electron-donating group (Fischer carbene, type V).²⁶

The first latent chelated catalysts, **1**, were reported by van der Schaaf et al. (Figure 2).²⁷ Later, Grubbs replaced the phosphine ligand by an N-heterocyclic carbene (NHC) to produce complex **2**. The *2-trans* isomer would revert to the more stable *2-cis* isomer, improving the latency of the precatalyst.²⁸ Other pioneering efforts in the area of chelating benzylidenes for latent ruthenium olefin metathesis precatalysts were reported by Slugovc, Grell, and their co-workers (precatalysts **3** and **4** and one of the first reported NHC-bearing precatalysts in a *cis*-dichloro configuration, **5**).²⁹ With an original approach, Barbasiewicz et al. exploited the steric effects of the benzylidene sixth position to tune the latency in O-chelated precatalysts **6–8**.³⁰

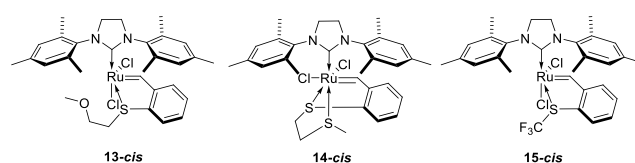


Figure 8. Tridentate sulfur-chelated complexes **13-cis** and **14-cis** and highly efficient metathesis catalyst **15-cis**.

SULFUR-CHELATED CATALYSTS: LATENT AND THERMOSWITCHABLE

In the group's first foray into this field, we envisioned that stronger ligation to the ruthenium center by a sulfur atom would generate a stable initiator.³¹ Unexpectedly, the new sulfur-chelated catalyst (**9-cis**) was isolated in a *cis*-dichloro geometry (Scheme 2). In this unusual configuration, the sulfur atom is not coordinated *trans* to the strongly σ -electron-donating NHC ligand; therefore, the *trans* influence is reduced, and the complex remains inactive at ambient temperatures.³² The isomeric kinetic product of this reaction, *9-trans*,³⁵ readily isomerized upon standing to the more stable *cis*-dichloro form (Scheme 3).

Catalyst **9-cis** exhibited exceptional stability (~ 20 days). In fact, heating a toluene solution of **9-cis** for 3 days at 90°C under air was required to significantly decompose the new catalyst. Its latency was first evaluated with the benchmark RCM reaction of diethyl diallylmalonate (DEDAM) (Figure 3). No conversion was observed after 1 week at room temperature. RCM could be induced by heating the reaction mixture to 80°C . The thermoswitchable behavior was demonstrated with intermittent periods of heating to 80°C and cooling to 25°C , and it was shown that RCM could be switched on and off even after more than 2 days.

9-cis was also tested for ROMP of dimethyl 5-norbornene-2,3-dicarboxylate.³⁴ As desired, no polymerization was observed at ambient temperature. Heating to 100°C initiated polymerization, and an unexpected thermoswitchable behavior was observed, also after more than 3 days of heating–cooling cycles (Figure 4).

Interestingly, the polydispersity indexes (PDIs) of the polymers obtained were noticeably lower than expected from a slow-initiating catalyst. This could be explained by a “turnover-limited polymerization” mechanism, where the degree of polymerization (DP) is controlled by the turnover number of the catalytic species and not by the ratio of monomer to initiator, as is common in living polymerization mechanisms.

PHOTOCHEMICAL ACTIVATION

Realizing that the isomerization process promotes activation of the sulfur-chelated precatalysts allowed us to imagine more efficient pathways for stimulation. On the basis of early reports on photoactive $\text{RuCl}_2(\text{DMSO})_4$ complexes,³⁵ we hypothesized that the sulfur–ruthenium bond could be dissociated by applying

Table 1. UV-Activated ROMP with Catalysts **10-cis** and **11-cis**^a

Entry	Monomer	Catalyst	PDI	Initiation Efficiency	Z/E	$M_n \times 10^5$	Conv. (%)
1		10-cis	1.5	0.10	1.7	2.5	40
		11-cis	1.5	0.17	1.7	2.5	66
2		10-cis	1.3	0.29	2.9	1.1	96
		11-cis	1.2	0.25	3.1	1.3	99
3		10-cis	1.4	0.55	1.1	0.5	86
		11-cis	1.5	0.39	1.2	0.7	84

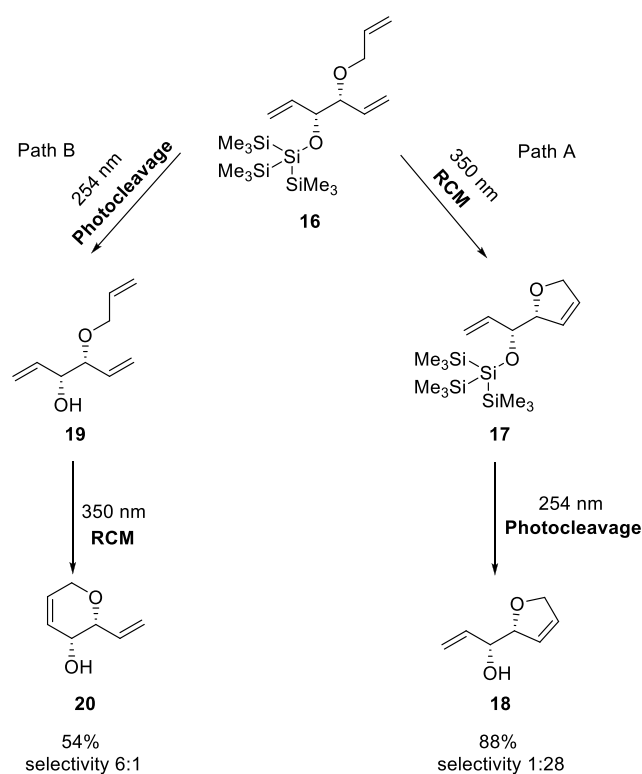
^aConversions were calculated using GC–MS after 24 h. Conditions: 0.5 M monomer in CH_2Cl_2 ; $[\text{monomer}]/[\text{cat.}] = 300$. M_n and PDI values were determined by triple-detector size-exclusion chromatography; Z/E values were determined by ^1H NMR spectroscopy.

Table 2. Comparative RCM and ROMP Activities of 9-*cis* and 15-*cis*^a

Entry	Substrate	Irradiation	Temp. (°C)	Time (h)	Cat. (mol %)	Conv. with 9- <i>cis</i> (%)	Conv. with 15- <i>cis</i> (%)
1		none	80	1	1	5	75
		none	30	2	0.5	<1	<1
		350 nm	30	2	0.5	<1	86
2		none	~35	24	0.3	<1	<1
		none	80	1.5	0.3	32	91
		350 nm	~35	1	0.3	<1	94

^aConversions were measured using GC-MS.

Scheme 5. Regioselective Chromatic-Orthogonal Ring-Closing Metathesis



UV irradiation. Initial attempts with catalyst 9-*cis* using a medium-pressure mercury UV-A lamp (100 W, 365 nm) were unsuccessful. However, addition of a suitable chromophore on the thioether increased the photosensitivity of the complex. Thus, complexes 10-*cis*, 11-*cis*, and 12-*cis* were designed and synthesized (Figure 5).^{1,36}

The photoactivity of the precatalysts was studied by irradiating a DEDAM solution in the presence of each catalyst. Indeed, the aromatic substitution on the thioether resulted in greatly increased efficiency for photoactivation, and 10-*cis* provided the best results with almost 90% conversion (Figure 6).

The suggested mechanism for photoactivation is shown in Scheme 4. Irradiation of 10-*cis* forms an unstable 14-electron *cis* transition state (10-*cis* 14e⁻) that quickly rearranges to the more stable 14-electron *trans* intermediate (10-*trans* 14e⁻), which was then capped by the sulfur atom to afford the stable metathesis-active 16-electron *trans* precatalyst (10-*trans*).

The switchable nature of the system was demonstrated by 15 min irradiation of a tetrachloroethane solution of DEDAM with 5 mol % catalyst 11-*cis* (activation), followed by 5 min

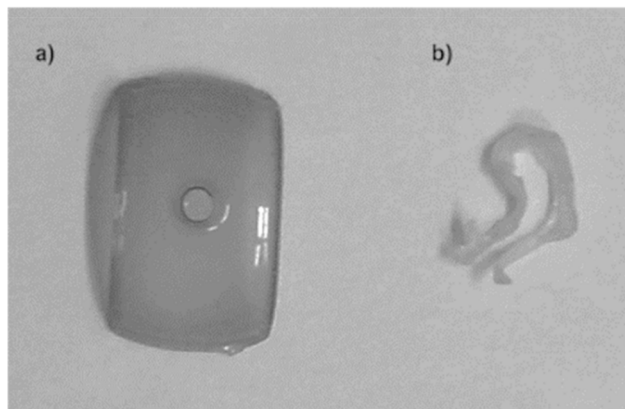
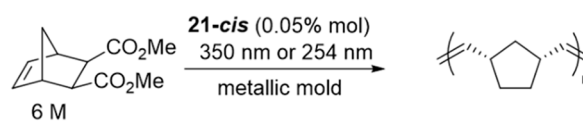
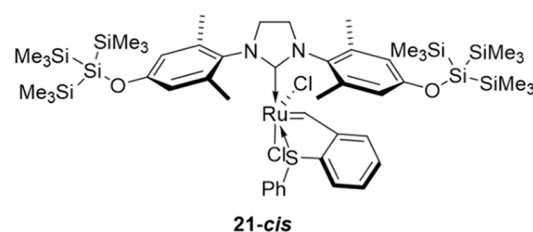
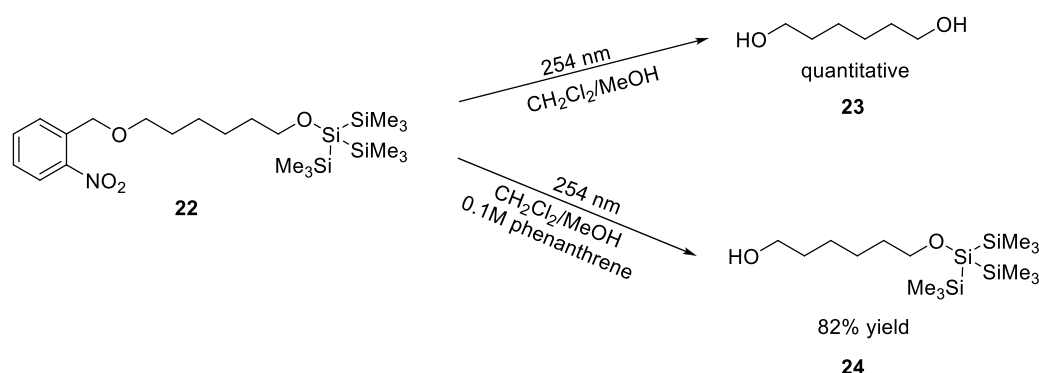


Figure 9. (top) Sulfur-chelated photoswitchable catalyst 21-*cis* with a chromatic-orthogonal “kill-switch”. (bottom) Polymerization of a norbornene derivative in metal molds with 21-*cis*: (a) irradiation at 350 nm; (b) irradiation at 254 nm followed by UV-A. Reproduced with permission from ref 41. Copyright 2016 Wiley-VCH.

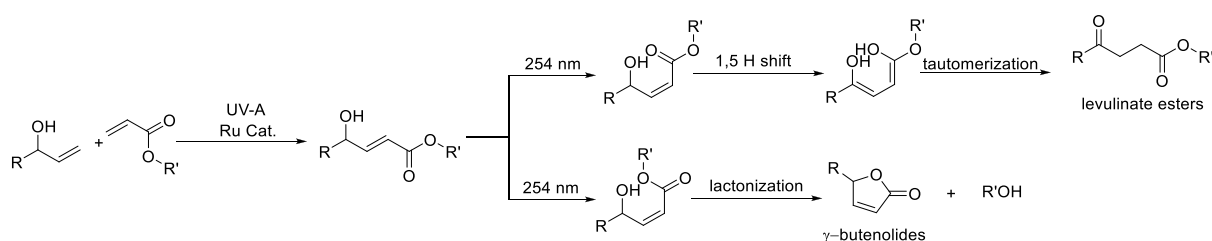
heating at 80 °C (deactivation). In a counterintuitive fashion, heating the active *trans* isomer (out of equilibrium as a result of the irradiation) accelerates thermal isomerization back to the more stable *cis* form and reduces the amount of active precatalyst. Thus, the metathesis reaction is promoted by irradiation and actually stopped by heating for a short time (naturally, continued heating would provide a steady supply of active *trans* isomer to continue the reaction). The photoinduced metathesis activity of the most efficient complexes was further evaluated with several RCM and ROMP reactions (Figure 7 and Table 1).

Although they showed improved performances compared with 9-*cis*, this new generation of thermally and photochemically switchable sulfur-chelated catalysts still suffered from some drawbacks. The complexes were still not active enough to accomplish metathesis reactions of “difficult” substrates, and even relatively simple reactions required high precatalyst loadings to reach completion. Moreover, highly reactive ROMP monomers such

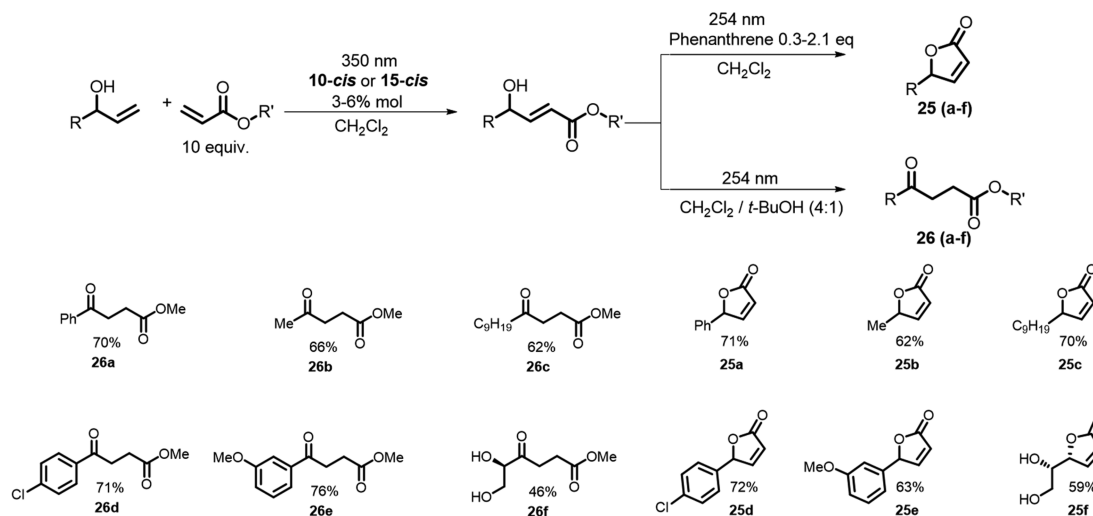
Scheme 6. Selective Photodeprotection of a 2-Nitrobenzyl PPG in the Presence of a Supersilyl Using Phenanthrene as a Molecular UV Filter



Scheme 7. Divergent Photochemical Reactions to Form Butenolides and Levulinates



Scheme 8. All-Photochemical Divergent Syntheses of Butenolides (25a–f) and Levulinates (26a–f)



as norbornene (NB) and dicyclopentadiene (DCPD) were polymerized by **10-cis** and **11-cis** at ambient temperatures and in the dark (no latency). In view of these deficiencies, new systems were sought to widen the latency gap and improve the catalytic activity. Complexes **13-cis** and **14-cis** were designed to be extremely dormant precatalysts by using a three-point chelation. In contrast, complex **15-cis** was designed to be a more efficient catalyst in its active form because of the strong electron-withdrawing influence of the trifluoromethyl substituent (Figure 8).

Contrary to expectations, **13-cis** did not form a three-point chelate with the ruthenium metal center. Indeed, its activity did not differ by much from those of the other sulfur-chelated catalysts previously reported. On the other hand, complex **14-cis** was chelated by both sulfur atoms. As expected, this complex was extremely dormant, showing latency for DCPD at ambient

temperatures; however, this strategy turned out to be a double-edged sword, as its metathesis activity was very poor (only 37% conversion in ROMP of DCPD after 3 h at 110 °C).

Catalyst **15-cis** is a true success story. This catalyst was latent at room temperature but displayed much-superior activity when activated (see the comparison with catalyst **9-cis** in Table 2), especially in photoinduced reactions.

GUIDING CHEMISTRY WITH LIGHT

The extensive work of Bochet and co-workers on the development of chromatic-orthogonal systems,^{18,37} i.e., systems in which two photochemical reactions can be executed commutatively using different colors of light, and the pioneering works on molecular photoswitches by Feringa and others³⁸ highlighted the elegance and simplicity of guiding a reaction

Scheme 9. Synthesis of the Marine Product Isocladospolide B Using a Photochemical Divergent Protocol

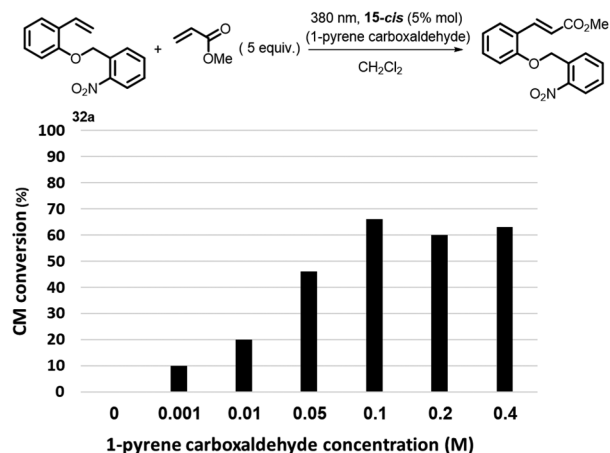
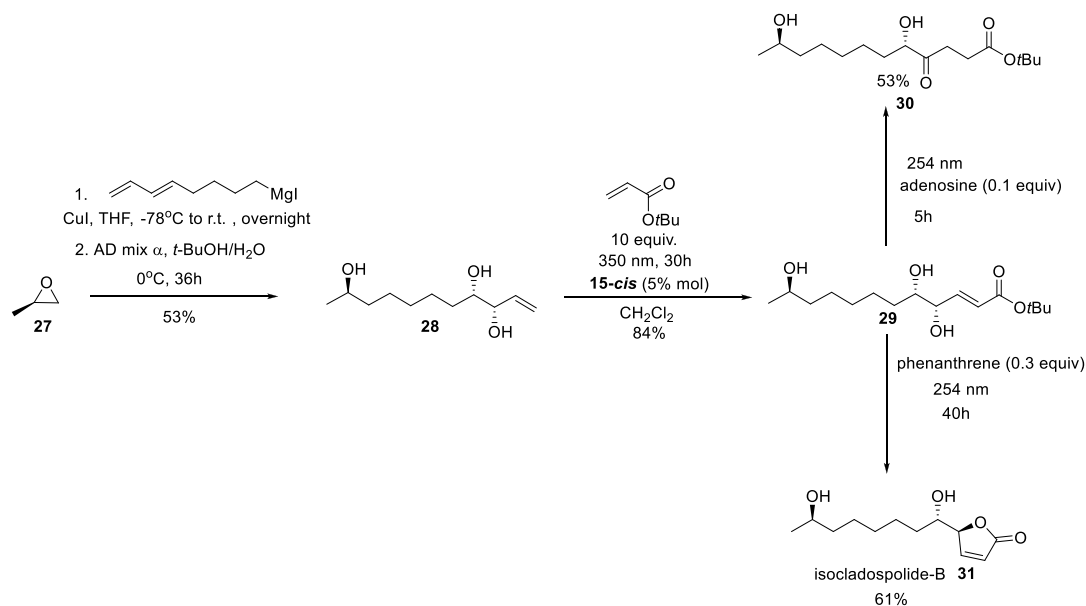


Figure 10. UV-filter-enabled cross-metathesis of 2-nitrobenzylvinyl-phenol and methyl acrylate with different concentrations of pyrene-1-carboxaldehyde as the UV filter.

outcome by using only light. The unique photoswitchable activity displayed by the sulfur-chelated metathesis catalysts provided the perfect opportunity to extend the concept of chromatic orthogonality to catalytic olefin metathesis reactions, asking the question “would it be possible to toggle between two different olefin metathesis products by using only light?”

Inspired by the studies of Schmidt and Nave on regioselective RCM reactions,³⁹ triene **16** was designed (Scheme 5).² Accordingly, **16** could form a five-membered-ring or a six-membered-ring product depending on steric hindrance. Thus, a method was sought to promote a process that would result in significant steric volume differences by irradiation with a light source that would not induce olefin metathesis. Indeed, while the catalysts (**10-cis** or **11-cis**) were sensitive to UV-A light, a bulky supersilyl group could be selectively photocleaved only with UV-C.⁴⁰ Thus, when the metathesis reaction was initiated in the presence of the bulky supersilyl group (path A, 350 nm followed by 254 nm), a five-membered ring (**17**) was preferentially formed. Alternatively, when the metathesis reaction was triggered after the cleavage of the supersilyl group (path B,

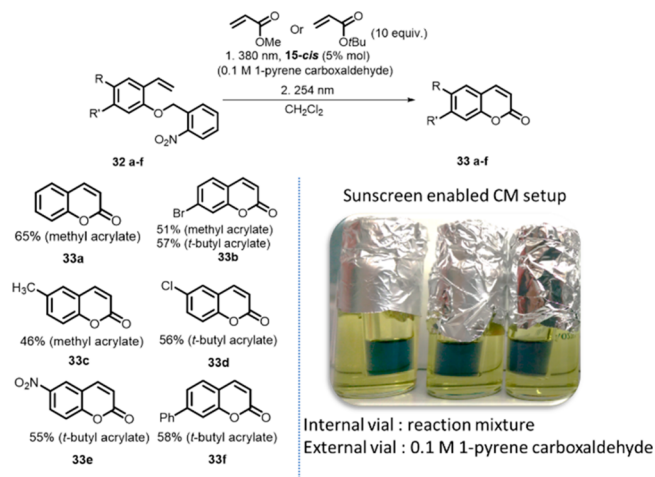
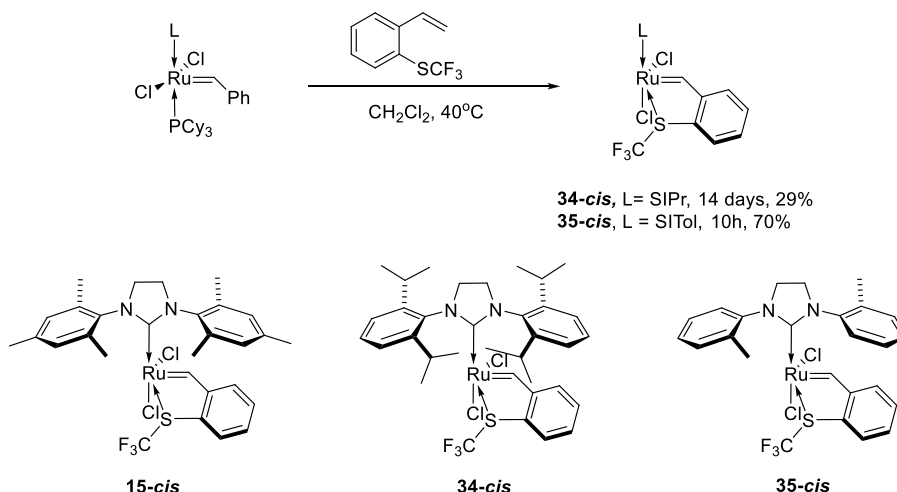
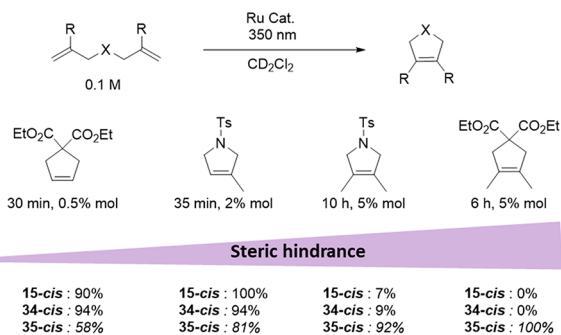


Figure 11. (left) Two-step photochemical synthesis of coumarins via sunscreen-enabled olefin metathesis (isolated yields are shown). (right) Reaction setup of the sunscreen-enabled cross-metathesis. The inner vial contains the olefin metathesis mixture, and the external vial contains a 0.1 M pyrene-1-carboxaldehyde solution.

254 nm followed by 350 nm), RCM to give a six-membered ring (**20**) was favored.

The inherent chromatic orthogonality displayed between the isomerization reaction of the sulfur-chelated catalysts (photoactivation) and the removal of supersilyl ethers was further exploited in the design of a catalyst with an embedded self-destruction function, **21-cis**.⁴¹ Although destruction of an active catalyst may seem to be a waste of a precious rare-metal catalyst, this function could be of great use in stereolithography, especially in layer-by-layer 3D printing processes. “Killing” the remaining active catalyst after polymerization and before applying a new layer of monomer/catalyst mixture may help in preventing loss of spatial resolution. In this design, the photosensitive supersilyl groups were directly installed on the NHC ligand (Figure 9, top). Thus, olefin metathesis was induced by the precatalyst upon exposure to 350 nm light, while exposure to 254 nm light led to its rapid decomposition (Figure 9, bottom).

Scheme 10. Synthesis of SCF₃-Chelated Complexes with the NHC Ligands SIPr (34-*cis*) and SITol (35-*cis*)Scheme 11. Photoinduced RCM of Substrates with Increasing Steric Bulk Using 15-*cis*, 34-*cis*, and 35-*cis*^a

^aConversions were measured by ¹H NMR spectroscopy.

SUNSCREEN-ENABLED PHOTOINDUCED OLEFIN METATHESIS

The regioselective chromatic-orthogonal sequence used with triene **16** disclosed an unanticipated difficulty. The removal of the supersilyl protecting group was hampered because of the presence of the ruthenium catalyst (which strongly absorbs UV-C), and it took great skill to find the right conditions in order to achieve the desired chromatic-orthogonal sequence.

One of the major drawbacks of organic photochemical reactions is their poor selectivity. Often such reactions result in the formation of several products, and it is very difficult to control the selectivity for one product over the others. Thus, this “sunscreen” effect was harnessed to develop a methodology for the selective removal of photolabile protecting groups (PPGs).⁴² The method relies on the difference between the molar absorption

coefficients (at similar wavelengths) of a pair of PPGs and utilizes auxiliary strongly absorbing molecules that overlap the specific absorbance of the PPGs. Thus, 2-nitrobenzyl-protected alcohols were selectively photocleaved in the presence of strongly UV-C-absorbing phenanthrene, while supersilyl ethers remained unscathed (Scheme 6). The UV filter could be applied as an additive or, more conveniently, as an external solution, bypassing the need for additional purification of the reaction products.

The scope of the sunscreen method was further studied with different types of photochemical reactions. The cross-metathesis product of allylic alcohols and acrylates can further react photochemically by two competing pathways to afford different organic scaffolds: butenolides and levulinates. The first reaction path involves a *trans/cis* double-bond isomerization followed by an intramolecular lactonization to produce the butenolide. The key step in the alternative pathway is a 1,5-hydrogen shift and subsequent tautomerization to form the levulinate (Scheme 7).

Under regular conditions, both types of products are formed with very little selectivity. However, when phenanthrene was added to the reaction mixture, the 1,5-hydrogen shift was completely blocked, allowing selective formation of butenolides. Without phenanthrene, the selectivity could be shifted to produce the levulinate esters. Thus, a protocol for a selective photochemical divergent two-step conversion of allylic alcohols and acrylates to butenolides and levulinates was successfully accomplished, as detailed in Scheme 8. Moreover, by the use of this photochemical protocol, the total synthesis of the marine natural product isocladospolide B could be achieved with very high efficiency (Scheme 9).

Another challenge that could be addressed using the sunscreen methodology is the cross-metathesis reaction of

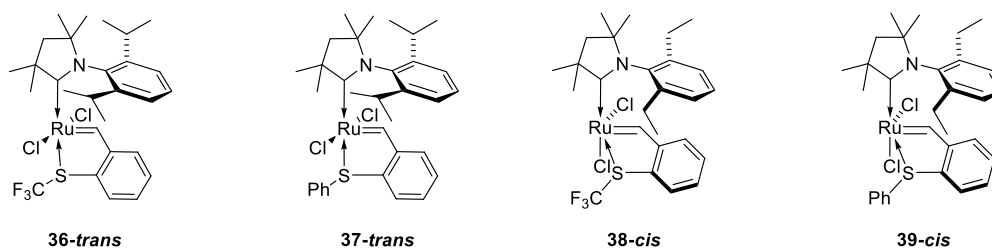


Figure 12. CAAC-bearing sulfur-chelated metathesis precatalysts.

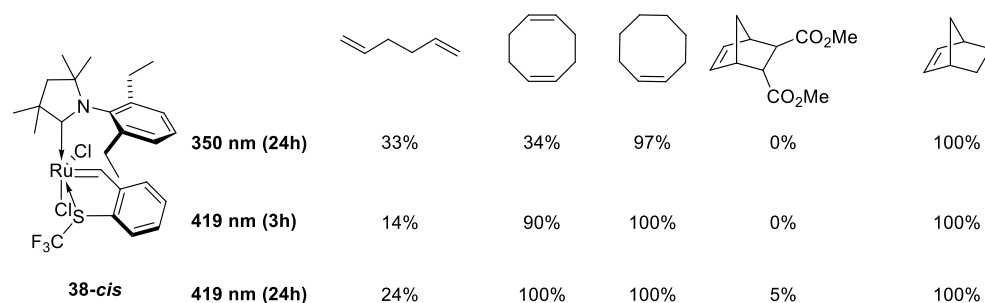
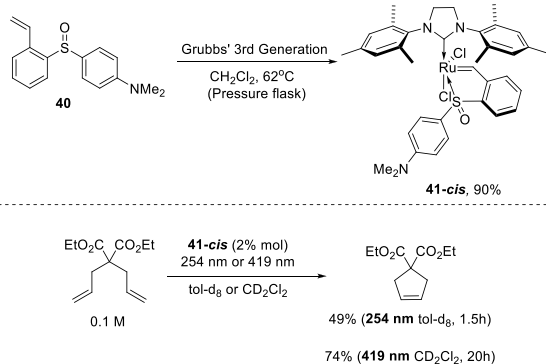


Figure 13. Photocatalytic activity of **38-cis**. Reaction conditions: **38-cis** loading, 0.1% mol; monomer concentration, 0.5 M.

Scheme 12. Photoactivity of **41-cis**



2-vinylphenols. When coordinated to the ruthenium catalyst, these substrates form a stable chelate and inhibit catalysis. Thus, we adopted a sunscreen effect solution to this problem. A UV-A PPG with low absorption could “survive” photoinduced activation of a ruthenium catalyst if a suitable molecular UV filter is procured. 2-Nitrobenzyl was selected to be the protecting group for the phenols on the basis of its relatively low absorption in the UV-A region. In this case, pyrene-1-carboxaldehyde, a dye with strong absorption in the UV-A and visible regions, was chosen as the UV filter. Thus, cross-metathesis of 2-nitrobenzyl-protected vinylphenol with methyl acrylate was investigated with catalyst **15-cis** and 380 nm irradiation in the presence of an external solution of pyrene-1-carboxaldehyde at different concentrations (Figure 10). As can be clearly observed, in the absence of pyrene-1-carboxaldehyde, the 2-nitrobenzyl PPG was removed and catalysis was inhibited. Increasing the dye concentration resulted in improved reaction conversions up to a concentration of 0.1 M, where the “protective” effect leveled off.

This approach was exploited in an all-photochemical synthesis of coumarins. The first step was cross-metathesis between 2-nitrobenzyl-protected vinylphenols (**32**) and acrylates in the presence of pyrene-1-carboxaldehyde. This was followed by removal of the external filter solution and irradiation with 254 nm light to trigger a chain of three photochemical reactions: removal

of the 2-nitrobenzyl PPG, then trans to cis double-bond isomerization, and finally cyclization to furnish the coumarins (Figure 11).

■ EXPLORING THE EFFECTS OF ALTERING THE N-HETEROCYCLIC CARBENE LIGAND

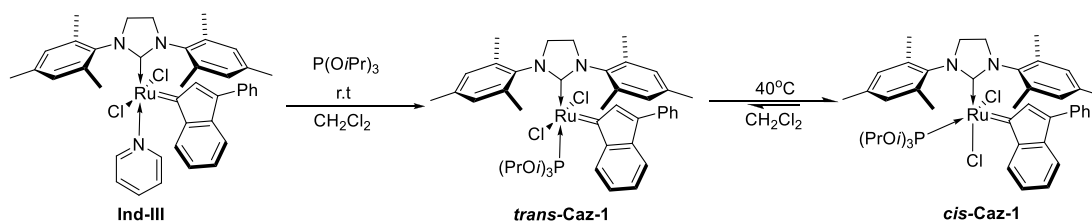
The fine balance between the latency and augmented catalytic activity of **15-cis** was the driving force for further investigation of the potential of SCF₃-type chelated systems. The variation of the steric and electronic properties of NHC ligands is well-known to have a large impact on the activity of ruthenium metathesis catalysts.⁴³ For example, 1,3-bis(2,6-diisopropylphenyl)imidazolidin-2-ylidene (SIPr) (Scheme 10) was found to increase the thermal stability and activity of metathesis complexes for terminal olefins.⁴⁴ On the other hand, NHC ligands with smaller volumes, such as 1,3-bis(2-methylphenyl)imidazolidin-2-ylidene (SITol) (Scheme 10), are known to improve the RCM of sterically demanding substrates.⁴⁵

Thus, the effect of different NHC ligands with varying steric bulk on the activity of sulfur-chelated switchable metathesis catalysts was also studied.⁴⁶ **34-cis** and **35-cis**, bearing a SIPr and SITol ligand, respectively, were prepared, and their activities in olefin metathesis reactions were compared to that of **15-cis** (Scheme 10).

It is noteworthy that the synthesis of **34-cis** required a long reaction time (3 weeks), as the steric congestion associated with the SIPr ligand significantly increased the energy barrier for trans–cis isomerization. With the catalysts in hand, the thermal and photochemical behavior toward a set of RCM reactions (disubstituted to tetrasubstituted) was studied. As expected, the catalyst with the bulkier NHC showed superior activity toward the RCM reaction of terminal diolefins, while the catalyst with the sterically lighter NHC promoted the photoinduced metathesis of tetrasubstituted RCM reactions in high yields. To date, **35-cis** is the only photoswitchable catalyst that can efficiently promote tetrasubstituted RCM reactions (Scheme 11).

In 2005 Bertrand and co-workers introduced cyclic alkyl amino carbene (CAAC) ligands as strong electron-donating

Scheme 13. Synthesis of the Catalyst **cis-Caz-1**



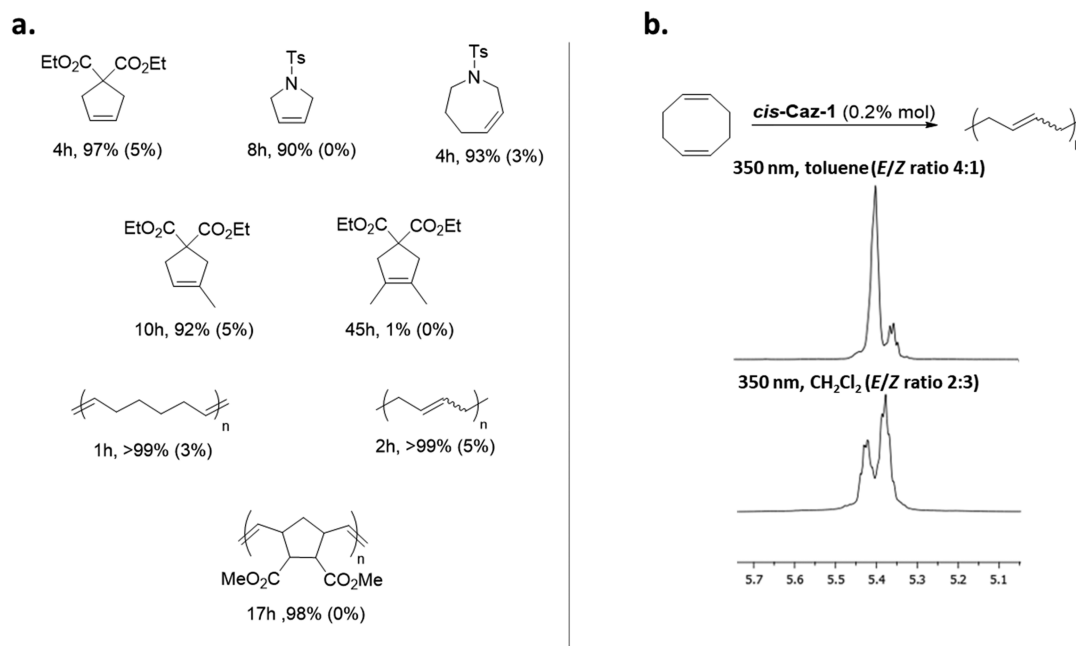


Figure 14. (a) Photoinduced RCM and ROMP reactions with *cis*-Caz-1 at 350 nm. Dark control conversions are given in parentheses. RCM conditions: 0.1 M substrate and 1% mol catalyst in dichloromethane. ROMP conditions: 0.5 M monomer and 0.2 mol % catalyst in dichloromethane. (b) Solvent effect in photopolymerization of COD. The trans-rich polymer is obtained in toluene (top), and the cis-rich polymer is obtained in dichloromethane (bottom).

ligands for transition metal catalysis.⁴⁷ The first ruthenium olefin metathesis catalysts bearing CAAC ligands were reported by Grubbs and Bertrand just 2 years later.⁴⁸ These complexes were found to be extremely stable and efficient catalysts⁴⁹ and also to prevent undesired olefin migration reactions at elevated temperatures.⁵⁰ More recently, a new generation of CAAC complexes was reported by Skowerski and Fogg showing exceptional catalytic efficiency and remarkable stability.⁵¹ To examine the effect of CAAC ligands on sulfur-chelated complexes, four new sulfur-chelated complexes bearing CAAC ligands were prepared (Figure 12).⁵²

Unexpectedly, the complexes prepared using a bulky 1,3-diisopropylphenyl CAAC ligand (**36-trans** and **37-trans**) were isolated in the *trans*-dichloro configuration as the thermodynamically stable form. However, these complexes could not promote photoinduced olefin metathesis reactions and only reacted thermally with highly reactive monomers. Conversely, complexes **38-cis** and **39-cis** with reduced steric pressure from the CAAC ligand were found to be efficient metathesis catalysts (when activated). While complex **39-cis** was inactive with light stimulation, **38-cis** showed good activity with 350 and 419 nm light, completing a variety of polymerization reactions (Figure 13).

■ PHOTOACTIVE CHELATED SULFOXIDE CATALYSTS

In an attempt to tune the reactivity of novel sulfur-chelated catalysts, our group as well as the group of Grela investigated the effect of oxidizing the sulfur atom to a sulfoxide.⁵³ However, given the much weaker electron donation of the oxidized sulfur, the chelated complexes obtained were more stable in the *trans*-dichloro configuration and thus were metathesis-active at ambient temperatures. We hypothesized that by adding a strongly electron-donating group on the chelating aryl sulfoxide, the electron density on the coordinating sulfur atom may force it to a *cis*-dichloro geometry to avoid the stronger *trans* influence from the NHC

ligand.⁵⁴ Thus, styrene **40** was prepared and reacted with Grubbs' third-generation catalyst to give **41-cis** (Scheme 12, top).

41-cis was indeed latent toward RCM and polymerization reactions at room temperature and could be thermally activated at 80 °C in toluene. As sulfoxide ligands possess rich photochemistry,³⁵ the photoactivity of this latent complex was investigated. Interestingly, in toluene, the complex was activated with 254 nm light; unfortunately, the high-energy light also led to rapid decomposition of the catalyst and poor metathesis efficiency. When the solvent was replaced by dichloromethane, photoactivity was observed at 419 nm. However, despite (or maybe because of) the excellent latency of this catalyst, its catalytic activity was somewhat limited (Scheme 12, bottom).

■ PHOTOACTIVATION OF RUTHENIUM PHOSPHITE COMPLEXES FOR OLEFIN METATHESIS

Ruthenium-based metathesis catalysts stabilized by phosphite ligands were first introduced by Cazin and co-workers in 2010.²¹ By the reaction of an indenylidene complex (**Ind-III**) with triisopropyl phosphite, *trans*-Caz-1 was obtained. In boiling dichloromethane, this complex isomerized to the thermodynamically stable *cis*-dichloro configuration, known as *cis*-Caz-1 (Scheme 13). *cis*-Caz-1 showed latency toward several olefin metathesis substrates at ambient temperature and could be switched on thermally in hot toluene (80 °C) to promote the catalysis of sterically demanding RCM reactions under air with minimal catalyst loadings.⁵⁵

The resemblance of the isomerization behavior of *cis*-Caz-1 to that of the sulfur-chelated catalysts, combined with fact that this was not a chelated catalyst, drew our attention toward the possibility of disrupting the Ru–P bond by using light. Indeed, *cis*-Caz-1 was found to be readily activated under UV-A light (350 nm), becoming the first (and to date only) commercially available photoswitchable metathesis catalyst, making photoinduced olefin metathesis widely accessible.³ The light-induced

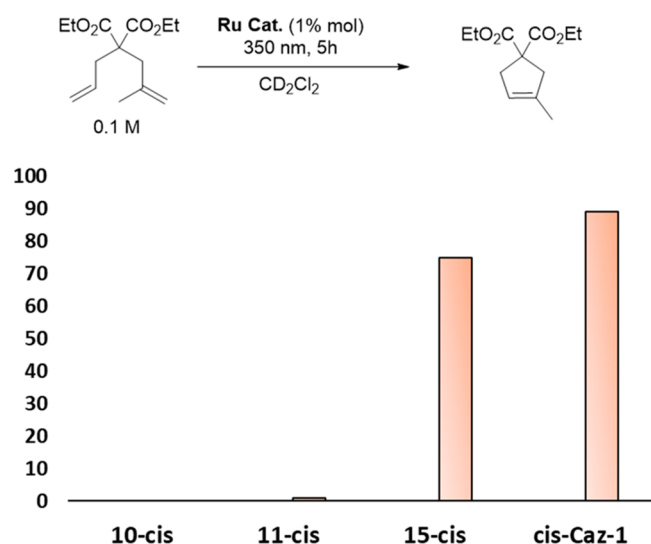
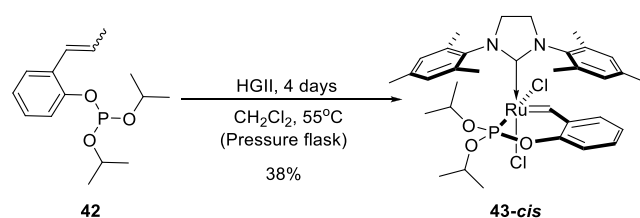


Figure 15. Comparison between sulfur-chelated photoswitchable catalysts **10-cis**, **11-cis**, **15-cis**, and **cis-Caz-1**. Conversions were measured by ^1H NMR spectroscopy.

Scheme 14. Synthesis of **43-cis**



catalytic activity of **cis-Caz-1** was thoroughly studied and showed great competence for a variety of ROMP, RCM, and CM reactions (Figure 14a). The study of ROMP of 1,5-cyclooctadiene (COD) using **cis-Caz-1** disclosed an intriguing solvent effect (Figure 14b). When light-induced polymerization was carried out in dichloromethane, a *cis*-rich polymer was obtained and isolated (3:2 *cis*:*trans* ratio in the polymer). However, when the same reaction was carried out in toluene, the resulting polymer had the expected thermodynamic ratio of 4:1 in favor of *trans*.

The catalytic activity of **cis-Caz-1** was compared to that of the state-of-the-art photoactive sulfur-chelated metathesis precatalysts using a model RCM reaction (Figure 15).

When Cazin et al. tried to install phosphite ligands on Grubbs benzylidenes, only complexes in a *trans*-dichloro configuration were obtained.⁵⁶ As expected, these catalysts were metathesis-active at ambient temperatures. On the basis of a previous study on chelating phosphine ligands,⁵⁷ we surmised that a chelating benzylidene phosphite ligand would force a *cis*-dichloro configuration. Thus, **42** was synthesized and reacted with the Hoveyda–Grubbs second-generation catalyst to afford complex **43-cis** (Scheme 14).³

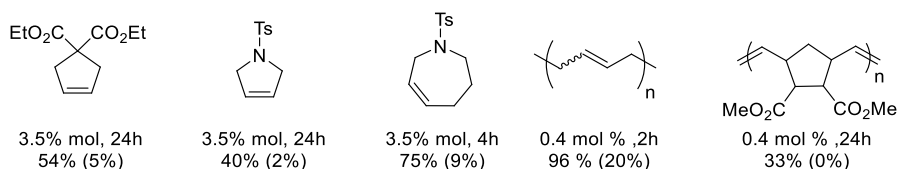


Figure 16. Catalytic activity of **43-cis** with a 405 nm LED.

Scheme 15. Synthesis of Complexes **46-cis** and **47-cis**

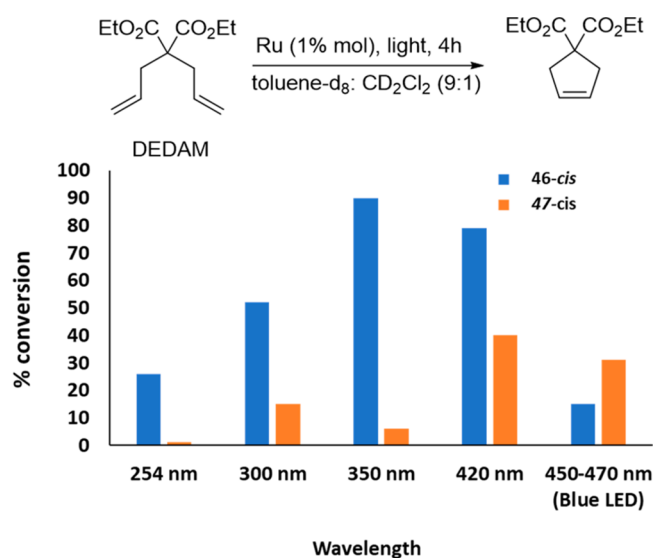
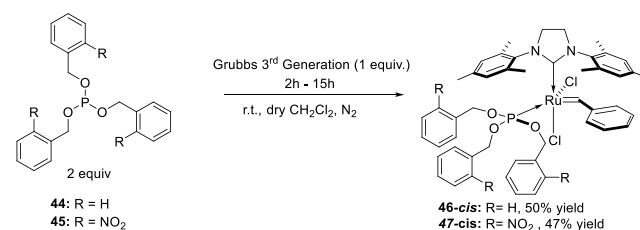


Figure 17. Photoactivities of **46-cis** and **47-cis** at different wavelengths.

The *cis*-dichloro configuration of **43** was verified by NMR spectroscopy and single-crystal X-ray diffraction. This catalyst could be activated thermally by heating to 80 °C in toluene or photochemically using a 405 nm light-emitting diode (LED) in toluene to complete several RCM and ROMP reactions; unfortunately, the strong chelation also impeded a high catalytic activity, and metathesis reactions using this catalyst required long irradiation times and high catalyst loadings (Figure 16).

In order to further our research on photoactive phosphite-containing ruthenium alkylidenes, the effect of the phosphite ligands was studied by changing the type of phosphite ligand used. Thus, two benzyl phosphite ligands, **44** and **45**, were prepared. Notably, ligand **45** was designed to provide an alternative chromatic-orthogonal kill switch. Phosphites **44** and **45** were reacted with Grubbs third-generation complex to give complexes **46-cis** and **47-cis**, respectively (Scheme 15).⁴ To our satisfaction and great surprise, both complexes adopted the latent *cis*-dichloro geometry.

The photochemical activities of these catalysts were benchmarked by RCM of DEDAM (Figure 17). Catalyst **46-cis** showed activity at all wavelengths tested but was most efficient with UV-A and visible light (420 nm). On the other hand, catalyst **47-cis** was best activated with 420 nm light and surprisingly even with blue

Table 3. Photoinduced Olefin Metathesis by Complexes **46-cis** and **47-cis** with 420 nm Light^a

entry	substrate	product	time (h)	loading (% mol)	catalyst	% conversion (dark control) ^b	M _n (g/mol) (M _w /M _n)
1			8	1	46-cis	92(4)	-
			8	2	47-cis	80 (14)	
2			8	1	46-cis	92(0)	-
			8	2	47-cis	86 (0)	
3			8	1	46-cis	73(6)	-
			8	2	47-cis	46 (3)	
4			8	1	46-cis	92(6)	-
			8	2	47-cis	80 (4)	
5			1	0.1	46-cis	100(4)	1.49 × 10 ⁴ (1.99)
			1	0.05	47-cis	94 (4)	1.67 × 10 ⁴ (2.01)
6			1	0.05	46-cis	94(5)	1.76 × 10 ⁵ (1.52)
			1	0.05	47-cis	97 (14)	1.65 × 10 ⁵ (2.05)
7			1	0.1	46-cis	100(40)	9.89 × 10 ⁵ (1.57)
			1	0.2	47-cis	100 (16)	6.62 × 10 ⁵ (1.66)
8			1	0.1	46-cis	95(0)	n.d. ^c
			1	0.2	47-cis	94 (3)	n.d. ^c

^aReaction conditions: RCM: 0.1 M substrate in 0.45 mL of toluene-*d*₈ and 0.05 mL of catalyst stock solution in CD₂Cl₂ were irradiated for 8 h. ROMP: 0.5 M monomer in 0.45 mL of toluene-*d*₈ and 0.05 mL of catalyst stock solution in CD₂Cl₂ were irradiated for 1 h. ^bDark control experiments were covered with aluminum foil. ^cNot determined because of polymer insolubility.

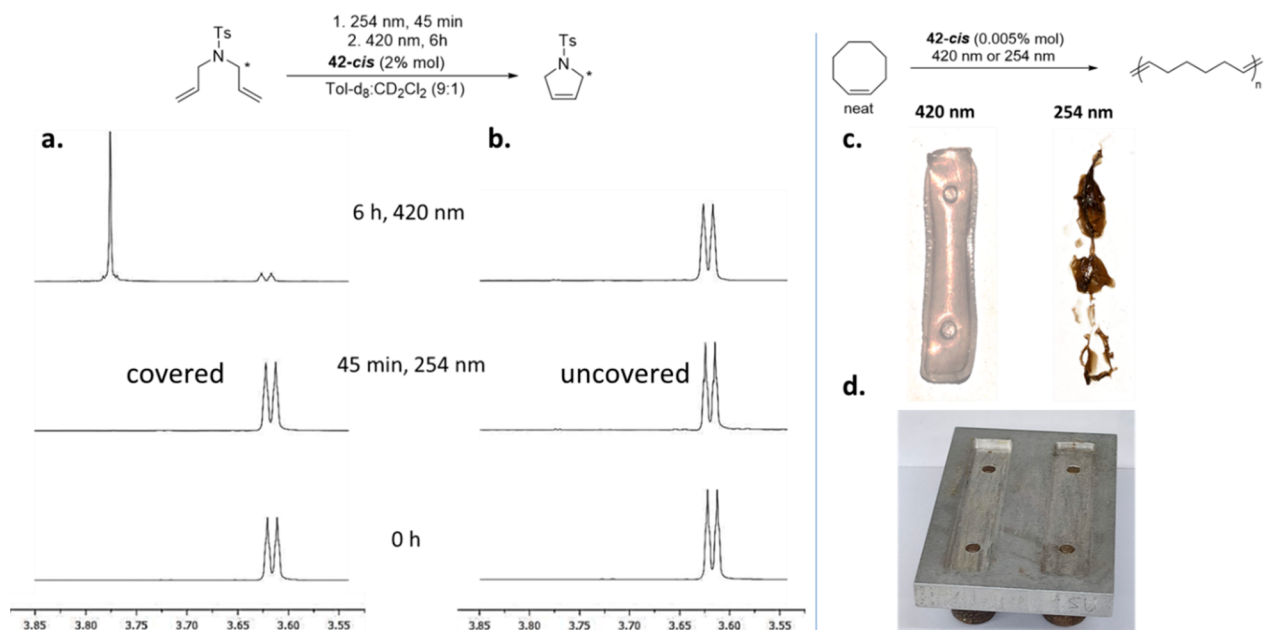


Figure 18. “Kill switch” efficiency of catalyst **47-cis**. (a, b) RCM of *N,N*-diallyltsylsulfonamide: (a) control experiment, in which the reaction mixture was covered during UV-C exposure; (b) the reaction mixture was exposed to UV-C, resulting in catalyst decomposition. (c) Photopolymerization of cyclooctene under irradiation at 420 and 254 nm. (d) the metal mold used for making the polymer films.

LED light (450–470 nm), but it was much less active under UV light because of the photosensitive nature of the 2-nitrobenzyl phosphite ligand, which led to catalyst decomposition (as expected).

The photoinduced olefin metathesis scope of **46-cis** and **47-cis** was studied in 420 nm light (Table 3). High catalytic efficiency under visible light and good latency with minimal reaction conversion in the dark control experiments were observed.

47-cis was designed with a chromatic-orthogonal self-destruct switch, similar to that of **21-cis**.⁴¹ The kill switch in this case is based on the photosensitivity of the 2-nitrobenzyl phosphite

ligand, and irradiation of **47-cis** with UV-C light led to rapid degradation of the catalyst. However, **47-cis** has additional advantages compared with **21-cis**. First, the activation with visible light is more efficient, and another important advantage is the straightforward and facile synthesis of the catalyst.⁵⁸ The efficiency of the kill switch was demonstrated with an RCM reaction. Two identical reaction mixtures were exposed to irradiation at 254 nm and then at 420 nm. During the exposure to UV-C light, the control experiment was covered with aluminum foil and afforded an 86% yield of the RCM product after exposure to visible light (Figure 18a). On the other hand,

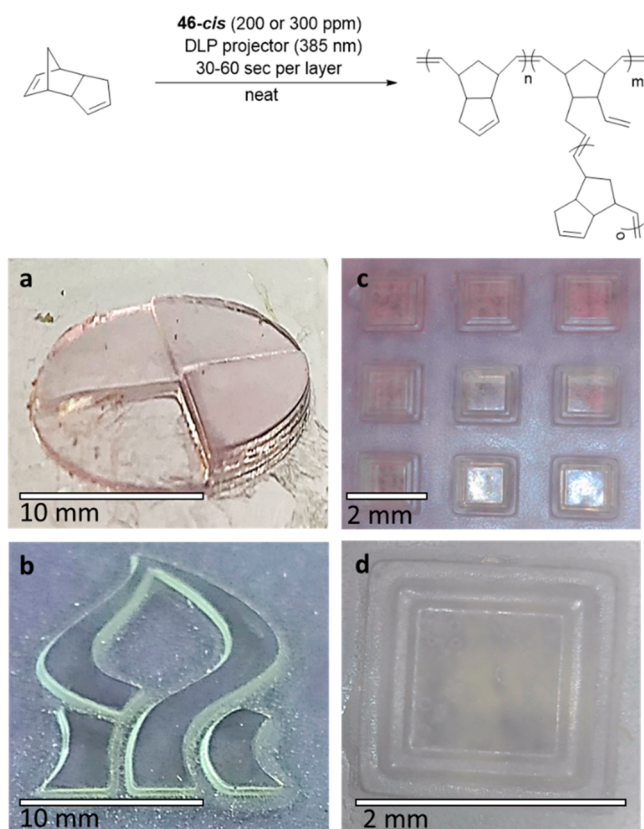


Figure 19. Light-induced stereolithography using catalyst **46-cis**. (a) Four layers: (i) full circle; (ii) three-fourth of a circle; (iii) half a circle; (iv) one fourth of a circle. (b) Ben-Gurion University of the Negev logo printed in two layers. The logo is used with permission from Ben-Gurion University of the Negev. (c) Pyramids consisting of three layers of decreasing size. (d) Zoom in on one pyramid from (c).

no conversion was observed in the experiment that was exposed to the UV-C light (Figure 18b). The kill switch was also tested in the ROMP of cyclooctene (Figure 18c,d). A monomer/precatalyst mixture was placed in metal molds and subjected to UV-C followed by UV-A irradiation or just to UV-A irradiation. While the experiment that was exposed to visible light yielded a functional and elastic polymer film, the experiment that was exposed first to UV-C yielded a sticky amorphous gel.

3D printing of metathesis-based polymeric materials using stereolithography is an attractive application that is making its first steps toward industrial implementation (e.g., polySpectra, a company founded by Raymond Weitekamp, specializes in additive manufacturing using olefin metathesis technology).⁵⁹ This is due to the excellent mechanical properties of metathesis-based polymers, such as poly-DCPD.^{7a,c,60} Currently, however, the most desirable monomers are often very reactive, and even highly latent catalysts fail to form processable and durable monomer/precatalyst liquid mixtures. Notably, Moore and co-workers added phosphites to mixtures of Grubbs second-generation catalyst and DCPD to create stable catalyst/monomer formulations with long “pot life” values.^{7b,d,61} Inspired by this work, we anticipated that the latent benzylidene phosphite catalysts would also form stable formulations with DCPD, as they already bear the “retarding” phosphite ligand. Indeed, mixing **46-cis** (0.02 or 0.03 mol %) with DCPD resulted in a stable formulation that could be processed for more than 4 h at room temperature (and longer times at lower temperatures). These DCPD/catalyst formulations were then used for light-induced

stereolithography using a digital light processing (DLP) projector (385 nm) for short exposure times (30–60 s per layer), exploiting the excellent spatial resolution obtained by the DLP projector and the short reaction times (Figure 19). This demonstrated the excellent suitability of photoswitchable latent phosphite complexes for these type of applications.

OUTLOOK AND CONCLUSIONS

This Account has surveyed our group’s activity in the design and development of latent photoswitchable metathesis catalysts during the past 12 years and their applications in photoinduced polymerizations and selective light-triggered olefin metathesis reactions. The serendipitous finding that sulfur chelation leads to latency by changing the complex’s geometry allowed advances in the area of light-induced olefin metathesis by selective disruption of the chelating bond with light. Since the first S-chelated photoswitchable catalyst report in 2009, the field of light-induced metathesis has grown significantly. Our own contributions, which have produced several novel ruthenium photoinduced catalysts, brought about new research in chromatic-orthogonal sequences, photochemical divergent syntheses, efficient 3D printing of metathesis polymers, and the use of a wide light spectrum ranging from UV-C to visible light. Future work will include studies of new activation methodologies (IR light, dual-wavelength activation) and achieving novel photoinduced selectivity by changing the anionic ligands and using new NHC ligands. Indeed, it has been a colorful journey, and this summary recounts the path taken toward developing light activation of olefin metathesis and hopefully will inspire future research toward the rainbow of opportunities that await in photochemical metathesis.

AUTHOR INFORMATION

Corresponding Author

N. Gabriel Lemcoff – Department of Chemistry and Ilse Katz Institute for Nanoscale Science and Technology, Ben-Gurion University of the Negev, Beer-Sheva 84105, Israel; orcid.org/0000-0003-1254-1149; Email: Lemcoff@bgu.ac.il

Authors

Or Eivgi – Department of Chemistry, Ben-Gurion University of the Negev, Beer-Sheva 84105, Israel; orcid.org/0000-0003-0997-1711

Ravindra S. Phatake – Department of Chemistry, Ben-Gurion University of the Negev, Beer-Sheva 84105, Israel; orcid.org/0000-0001-6046-1042

Noy B. Nechmad – Department of Chemistry, Ben-Gurion University of the Negev, Beer-Sheva 84105, Israel

Complete contact information is available at: <https://pubs.acs.org/10.1021/acs.accounts.0c00495>

Author Contributions

§O.E., R.S.P., and N.B.N. contributed equally.

Funding

This research was funded by the Israel Science Foundation (506/18).

Notes

The authors declare no competing financial interest.

Biographies

Or Eivgi is a postdoctoral fellow working with Professor Lemcoff. He obtained his Ph.D. in 2020 from Ben-Gurion University of the Negev under the supervision of Prof. Lemcoff. His current research focuses on developing new tools for photoinduced olefin metathesis.

Ravindra S. Phatake is a postdoctoral fellow working with Professor Lemcoff. He completed his Ph.D. in 2017 at CSIR-National Chemical Laboratory in Pune, India. His current research focuses on the design and synthesis of various monomers for ring-opening metathesis polymerization.

Noy B. Nechmad received her B.Sc. in 2017 and M.Sc. in 2019, both in Chemistry, from Ben-Gurion University of the Negev. Currently she is pursuing her Ph.D. under the supervision of Prof. Lemcoff, studying diiodo S-chelated olefin metathesis catalysts.

N. Gabriel Lemcoff received his Ph.D. in Chemistry in 2002 under the supervision of Prof. Benzion Fuchs. He then joined Prof. Steven C. Zimmerman at the University of Illinois at Urbana–Champaign and worked on molecularly imprinted dendrimers. In 2004 he joined the Chemistry Department at Ben-Gurion University of the Negev, where he is currently the Dean of the Faculty of Natural Sciences. In addition to working with polymers, light, and latent olefin metathesis catalysts, he is a fervent River Plate supporter.

REFERENCES

(1) Ben-Asuly, A.; Aharoni, A.; Diesendruck, C. E.; Vidavsky, Y.; Goldberg, I.; Straub, B. F.; Lemcoff, N. G. Photoactivation of Ruthenium Olefin Metathesis Initiators. *Organometallics* **2009**, *28*, 4652–4655.

(2) Levin, E.; Mavila, S.; Eivgi, O.; Tzur, E.; Lemcoff, N. G. Regioselective Chromatic Orthogonality with Light-Activated Metathesis Catalysts. *Angew. Chem., Int. Ed.* **2015**, *54*, 12384–12388.

(3) Eivgi, O.; Guidone, S.; Frenklah, A.; Kozuch, S.; Goldberg, I.; Lemcoff, N. G. Photoactivation of Ruthenium Phosphite Complexes for Olefin Metathesis. *ACS Catal.* **2018**, *8*, 6413–6418.

(4) Eivgi, O.; Vaisman, A.; Nechmad, N. B.; Baranov, M.; Lemcoff, N. G. Latent Ruthenium Benzyldiene Phosphite Complexes for Visible-Light-Induced Olefin Metathesis. *ACS Catal.* **2020**, *10*, 2033–2038.

(5) Higman, C. S.; Lummiss, J. A. M.; Fogg, D. E. Olefin Metathesis at the Dawn of Implementation in Pharmaceutical and Specialty-Chemicals Manufacturing. *Angew. Chem., Int. Ed.* **2016**, *55*, 3552–3565.

(6) (a) Sytniczuk, A.; Forcher, G.; Grotjahn, D. B.; Grela, K. Sequential Alkene Isomerization and Ring-Closing Metathesis in Production of Macrocyclic Musks from Biomass. *Chem. - Eur. J.* **2018**, *24*, 10403–10408. (b) Sytniczuk, A.; Leszczyńska, A.; Kajetanowicz, A.; Grela, K. Preparation of Musk-Smelling Macrocyclic Lactones from Biomass: Looking for the Optimal Substrate Combination. *ChemSusChem* **2018**, *11*, 3157–3166. (c) Ahmed, T. S.; Montgomery, T. P.; Grubbs, R. H. Using stereoretention for the synthesis of E-macrocycles with ruthenium-based olefin metathesis catalysts. *Chem. Sci.* **2018**, *9*, 3580–3583. (d) Nicola, T.; Brenner, M.; Donsbach, K.; Kreye, P. First Scale-Up to Production Scale of a Ring Closing Metathesis Reaction Forming a 15-Membered Macrocycle as a Precursor of an Active Pharmaceutical Ingredient. *Org. Process Res. Dev.* **2005**, *9*, 513–515. (e) Marx, V. M.; Herbert, M. B.; Keitz, B. K.; Grubbs, R. H. Stereoselective Access to Z and E Macrocycles by Ruthenium-Catalyzed Z-Selective Ring-Closing Metathesis and Ethanolysis. *J. Am. Chem. Soc.* **2013**, *135*, 94–97.

(7) (a) Kovačič, S.; Slugovc, C. Ring-opening metathesis polymerisation derived poly(dicyclopentadiene) based materials. *Mater. Chem. Front.* **2020**, *4*, 2235–2255. (b) Dean, L. M.; Wu, Q.; Alshangiti, O.; Moore, J. S.; Sottos, N. R. Rapid Synthesis of Elastomers and Thermosets with Tunable Thermomechanical Properties. *ACS Macro Lett.* **2020**, *9*, 819–824. (c) Trinh, T. K. H.; Schrodj, G.; Rigolet, S.; Pinaud, J.; Lacroix-Desmazes, P.; Pichavant, L.; Héroguez, V.;

Chemtob, A. Combining a ligand photogenerator and a Ru precatalyst: a photoinduced approach to cross-linked ROMP polymer films. *RSC Adv.* **2019**, *9*, 27789–27799. (d) Robertson, I. D.; Yourdkhani, M.; Centellas, P. J.; Aw, J. E.; Ivanoff, D. G.; Goli, E.; Lloyd, E. M.; Dean, L. M.; Sottos, N. R.; Geubelle, P. H.; Moore, J. S.; White, S. R. Rapid energy-efficient manufacturing of polymers and composites via frontal polymerization. *Nature* **2018**, *557*, 223–227.

(8) (a) Lummiss, J. A. M.; Oliveira, K. C.; Pranckevicius, A. M. T.; Santos, A. G.; dos Santos, E. N.; Fogg, D. E. Chemical Plants: High-Value Molecules from Essential Oils. *J. Am. Chem. Soc.* **2012**, *134* (46), 18889–18891. (b) Butilkov, D.; Lemcoff, N. G. Jojoba oil olefin metathesis: a valuable source for bio-renewable materials. *Green Chem.* **2014**, *16*, 4728–4733.

(9) Ogba, O. M.; Warner, N. C.; O’Leary, D. J.; Grubbs, R. H. Recent advances in ruthenium-based olefin metathesis. *Chem. Soc. Rev.* **2018**, *47*, 4510–4544.

(10) (a) Van Veldhuizen, J. J.; Garber, S. B.; Kingsbury, J. S.; Hoveyda, A. H. A Recyclable Chiral Ru Catalyst for Enantioselective Olefin Metathesis. Efficient Catalytic Asymmetric Ring-Opening/Cross Metathesis in Air. *J. Am. Chem. Soc.* **2002**, *124*, 4954–4955. (b) Ivry, E.; Ben-Asuly, A.; Goldberg, I.; Lemcoff, N. G. Amino acids as chiral anionic ligands for ruthenium based asymmetric olefin metathesis. *Chem. Commun.* **2015**, *51*, 3870–3873. (c) Hartung, J.; Dornan, P. K.; Grubbs, R. H. Enantioselective Olefin Metathesis with Cyclometalated Ruthenium Complexes. *J. Am. Chem. Soc.* **2014**, *136*, 13029–13037. (d) Stenne, B.; Collins, S. K. Enantioselective Olefin Metathesis. In *Olefin Metathesis*; Grela, K., Ed.; John Wiley & Sons: Hoboken, NJ, 2014; pp 233–267.

(11) (a) Higman, C. S.; Nascimento, D. L.; Ireland, B. J.; Audörsch, S.; Bailey, G. A.; McDonald, R.; Fogg, D. E. Chelate-Assisted Ring-Closing Metathesis: A Strategy for Accelerating Macrocyclization at Ambient Temperatures. *J. Am. Chem. Soc.* **2018**, *140*, 1604–1607. (b) Mangold, S. L.; Grubbs, R. H. Stereoselective synthesis of macrocyclic peptides via a dual olefin metathesis and ethenolysis approach. *Chem. Sci.* **2015**, *6*, 4561–4569.

(12) (a) Dumas, A.; Tarrieu, R.; Vives, T.; Roisnel, T.; Dorcet, V.; Baslé, O.; Mauduit, M. A Versatile and Highly Z-Selective Olefin Metathesis Ruthenium Catalyst Based on a Readily Accessible N-Heterocyclic Carbene. *ACS Catal.* **2018**, *8*, 3257–3262. (b) Keitz, B. K.; Endo, K.; Patel, P. R.; Herbert, M. B.; Grubbs, R. H. Improved Ruthenium Catalysts for Z-Selective Olefin Metathesis. *J. Am. Chem. Soc.* **2012**, *134*, 693–699. (c) Endo, K.; Grubbs, R. H. Chelated Ruthenium Catalysts for Z-Selective Olefin Metathesis. *J. Am. Chem. Soc.* **2011**, *133*, 8525–8527. (d) Smit, W.; Koudriavtsev, V.; Occhipinti, G.; Törnroos, K. W.; Jensen, V. R. Phosphine-Based Z-Selective Ruthenium Olefin Metathesis Catalysts. *Organometallics* **2016**, *35*, 1825–1837. (e) Occhipinti, G.; Hansen, F. R.; Törnroos, K. W.; Jensen, V. R. Simple and Highly Z-Selective Ruthenium-Based Olefin Metathesis Catalyst. *J. Am. Chem. Soc.* **2013**, *135*, 3331–3334.

(13) Montgomery, T. P.; Ahmed, T. S.; Grubbs, R. H. Stereoretentive Olefin Metathesis: An Avenue to Kinetic Selectivity. *Angew. Chem., Int. Ed.* **2017**, *56*, 11024–11036.

(14) (a) Yasir, M.; Liu, P.; Tennie, I. K.; Kilbinger, A. F. M. Catalytic living ring-opening metathesis polymerization with Grubbs’ second- and third-generation catalysts. *Nat. Chem.* **2019**, *11*, 488–494. (b) Leitgeb, A.; Wappel, J.; Slugovc, C. The ROMP toolbox upgraded. *Polymer* **2010**, *51*, 2927–2946. (c) Choi, T.-L.; Grubbs, R. H. Controlled Living Ring-Opening-Metathesis Polymerization by a Fast-Initiating Ruthenium Catalyst. *Angew. Chem., Int. Ed.* **2003**, *42*, 1743–1746.

(15) (a) Monsaert, S.; Lozano Vila, A.; Drozdak, R.; Van Der Voort, P.; Verpoort, F. Latent olefin metathesis catalysts. *Chem. Soc. Rev.* **2009**, *38*, 3360–3372. (b) Jakobs, R. T. M.; Sijbesma, R. P. Mechanical Activation of a Latent Olefin Metathesis Catalyst and Persistence of its Active Species in ROMP. *Organometallics* **2012**, *31*, 2476–2481. (c) Tzur, E.; Lemcoff, N. G. Latent Ruthenium Catalysts for Ring Opening Metathesis Polymerization (ROMP). In *Handbook of Metathesis*; Wiley-VCH: Weinheim, Germany, 2015; pp 283–312. (d) Szadkowska, A.; Grela, K. Initiation at Snail’s Pace: Design and

Applications of Latent Olefin Metathesis Catalysts Featuring Chelating Alkylidene Ligands. *Curr. Org. Chem.* **2008**, *12*, 1631–1647.

(16) (a) Eivgi, O.; Lemcoff, N. G. Turning the Light On: Recent Developments in Photoinduced Olefin Metathesis. *Synthesis* **2018**, *50*, 49–63. (b) Vidavsky, Y.; Lemcoff, N. G. Light-induced olefin metathesis. *Beilstein J. Org. Chem.* **2010**, *6*, 1106–1119. (c) Lai, H.; Zhang, J.; Xing, F.; Xiao, P. Recent advances in light-regulated non-radical polymerisations. *Chem. Soc. Rev.* **2020**, *49*, 1867–1886.

(17) (a) Theunissen, C.; Ashley, M. A.; Rovis, T. Visible-Light-Controlled Ruthenium-Catalyzed Olefin Metathesis. *J. Am. Chem. Soc.* **2019**, *141*, 6791–6796. (b) Boydston, A. J.; Cao, B.; Nelson, A.; Ono, R. J.; Saha, A.; Schwartz, J. J.; Thrasher, C. J. Additive manufacturing with stimuli-responsive materials. *J. Mater. Chem. A* **2018**, *6*, 20621–20645. (c) Pinaud, J.; Trinh, T. K. H.; Sauvanier, D.; Placet, E.; Songsee, S.; Lacroix-Desmazes, P.; Becht, J.-M.; Tarabls, B.; Lalevée, J.; Pichavant, L.; Héroguez, V.; Chemtob, A. In Situ Generated Ruthenium–Arene Catalyst for Photoactivated Ring-Opening Metathesis Polymerization through Photolabile N-Heterocyclic Carbene Ligand. *Chem. - Eur. J.* **2018**, *24*, 337–341. (d) Ligon, S. C.; Liska, R.; Stampfl, J.; Gurr, M.; Mühlaupt, R. Polymers for 3D Printing and Customized Additive Manufacturing. *Chem. Rev.* **2017**, *117*, 10212–10290. (e) Weitekamp, R. A.; Atwater, H. A.; Grubbs, R. H. Photolithographic Olefin Metathesis Polymerization. *J. Am. Chem. Soc.* **2013**, *135*, 16817–16820.

(18) (a) Wong, C.-H.; Zimmerman, S. C. Orthogonality in organic, polymer, and supramolecular chemistry: from Merrifield to click chemistry. *Chem. Commun.* **2013**, *49*, 1679–1695. (b) Bochet, C. Chromatic Orthogonality in Organic Synthesis. *Synlett* **2004**, 2268.

(19) Diesendruck, C. E.; Iliashvsky, O.; Ben-Asuly, A.; Goldberg, I.; Lemcoff, N. G. Latent and Switchable Olefin Metathesis Catalysts. *Macromol. Symp.* **2010**, *293*, 33–38.

(20) (a) Sanford, M. S.; Love, J. A.; Grubbs, R. H. Mechanism and Activity of Ruthenium Olefin Metathesis Catalysts. *J. Am. Chem. Soc.* **2001**, *123*, 6543–6554. (b) Nelson, D. J.; Manzini, S.; Urbina-Blanco, C. A.; Nolan, S. P. Key processes in ruthenium-catalysed olefin metathesis. *Chem. Commun.* **2014**, *50*, 10355–10375.

(21) Bantreil, X.; Schmid, T. E.; Randall, R. A. M.; Slawin, A. M. Z.; Cazin, C. S. J. Mixed N-heterocyclic carbene/phosphite ruthenium complexes: towards a new generation of olefin metathesis catalysts. *Chem. Commun.* **2010**, *46*, 7115–7117.

(22) Allaert, B.; Dieltiens, N.; Ledoux, N.; Vercaemst, C.; Van Der Voort, P.; Stevens, C. V.; Linden, A.; Verpoort, F. Synthesis and activity for ROMP of bidentate Schiff base substituted second generation Grubbs catalysts. *J. Mol. Catal. A: Chem.* **2006**, *260*, 221–226.

(23) (a) Monsaert, S.; Ledoux, N.; Drozdak, R.; Verpoort, F. A highly controllable latent ruthenium Schiff base olefin metathesis catalyst: Catalyst activation and mechanistic studies. *J. Polym. Sci., Part A: Polym. Chem.* **2010**, *48*, 302–310. (b) Schmid, T. E.; Modicom, F.; Dumas, A.; Borré, E.; Toupet, L.; Baslé, O.; Mauduit, M. Latent ruthenium–indenylidene catalysts bearing a N-heterocyclic carbene and a bidentate picolinate ligand. *Beilstein J. Org. Chem.* **2015**, *11*, 1541–1546.

(24) Vidavsky, Y.; Anaby, A.; Lemcoff, N. G. Chelating alkylidene ligands as pacifiers for ruthenium catalysed olefin metathesis. *Dalton Trans.* **2012**, *41*, 32–43.

(25) (a) Gawin, A.; Pump, E.; Slugovc, C.; Kajetanowicz, A.; Grela, K. Ruthenium Amide Complexes – Synthesis and Catalytic Activity in Olefin Metathesis and in Ring-Opening Polymerisation. *Eur. J. Inorg. Chem.* **2018**, *2018*, 1766–1774. (b) Kozłowska, A.; Dranka, M.; Zachara, J.; Pump, E.; Slugovc, C.; Skowerski, K.; Grela, K. Chelating Ruthenium Phenolate Complexes: Synthesis, General Catalytic Activity, and Applications in Olefin Metathesis Polymerization. *Chem. - Eur. J.* **2014**, *20*, 14120–14125.

(26) Louie, J.; Grubbs, R. H. Metathesis of Electron-Rich Olefins: Structure and Reactivity of Electron-Rich Carbene Complexes. *Organometallics* **2002**, *21*, 2153–2164.

(27) van der Schaaf, P. A.; Kolly, R.; Kirner, H.-J.; Rime, F.; Mühlebach, A.; Hafner, A. Synthesis and reactivity of novel ruthenium carbene catalysts. X-ray structures of $[\text{RuCl}_2(\text{=CHSC}_6\text{H}_5)_2(\text{P}^i\text{Pr}_3)_2]$

and $[\text{RuCl}_2(\text{CHCH}_2\text{CH}_2\text{-C}_6\text{H}_4\text{N})(\text{P}^i\text{Pr}_3)]$. *J. Organomet. Chem.* **2000**, *606*, 65–74.

(28) Ung, T.; Hejl, A.; Grubbs, R. H.; Schrodi, Y. Latent Ruthenium Olefin Metathesis Catalysts That Contain an N-Heterocyclic Carbene Ligand. *Organometallics* **2004**, *23*, 5399–5401.

(29) (a) Barbasiewicz, M.; Szadkowska, A.; Bujok, R.; Grela, K. Structure and Activity Peculiarities of Ruthenium Quinoline and Quinoxaline Complexes: Novel Metathesis Catalysts. *Organometallics* **2006**, *25*, 3599–3604. (b) Gstrein, X.; Burtscher, D.; Szadkowska, A.; Barbasiewicz, M.; Stelzer, F.; Grela, K.; Slugovc, C. Ruthenium quinoline and quinoxaline complexes: Thermally triggered initiators for ring opening metathesis polymerization. *J. Polym. Sci., Part A: Polym. Chem.* **2007**, *45*, 3494–3500. (c) Slugovc, C.; Burtscher, D.; Stelzer, F.; Mereiter, K. Thermally Switchable Olefin Metathesis Initiators Bearing Chelating Carbenes: Influence of the Chelate's Ring Size. *Organometallics* **2005**, *24*, 2255–2258. (d) Slugovc, C.; Perner, B.; Stelzer, F.; Mereiter, K. Second Generation Ruthenium Carbene Complexes with a cis-Dichloro Arrangement. *Organometallics* **2004**, *23*, 3622–3626.

(30) (a) Basak, T.; Grudzień, K.; Barbasiewicz, M. Remarkable Ability of the Benzylidene Ligand To Control Initiation of Hoveyda–Grubbs Metathesis Catalysts. *Eur. J. Inorg. Chem.* **2016**, *2016*, 3513–3523. (b) Barbasiewicz, M.; Szadkowska, A.; Makal, A.; Jarzemska, K.; Woźniak, K.; Grela, K. Is the Hoveyda–Grubbs Complex a Vinylogous Fischer-Type Carbene? Aromaticity-Controlled Activity of Ruthenium Metathesis Catalysts. *Chem. - Eur. J.* **2008**, *14*, 9330–9337.

(31) Ben-Asuly, A.; Tzur, E.; Diesendruck, C. E.; Sigalov, M.; Goldberg, I.; Lemcoff, N. G. A Thermally Switchable Latent Ruthenium Olefin Metathesis Catalyst. *Organometallics* **2008**, *27*, 811–813.

(32) Diesendruck, C. E.; Tzur, E.; Ben-Asuly, A.; Goldberg, I.; Straub, B. F.; Lemcoff, N. G. Predicting the Cis-Trans Dichloro Configuration of Group 15–16 Chelated Ruthenium Olefin Metathesis Complexes: A DFT and Experimental Study. *Inorg. Chem.* **2009**, *48*, 10819–10825.

(33) Kadyrov, R.; Rosiak, A.; Tarabocchia, J.; Szadkowska, A.; Bieniek, M.; Grela, K. New Concepts in Designing Ruthenium-Based Second Generation Olefin Metathesis Catalysts and Their Application. In *Catalysis of Organic Reactions*; Prunier, M. L., Ed.; Chemical Industries 123; CRC Press: Boca Raton, FL, 2009; pp 217–222.

(34) Diesendruck, C. E.; Vidavsky, Y.; Ben-Asuly, A.; Lemcoff, N. G. A latent s-chelated ruthenium benzylidene initiator for ring-opening metathesis polymerization. *J. Polym. Sci., Part A: Polym. Chem.* **2009**, *47*, 4209–4213.

(35) (a) Alessio, E.; Mestroni, G.; Nardin, G.; Attia, W. M.; Calligaris, M.; Sava, G.; Zorzet, S. Cis- and trans-dihalotetrakis(dimethyl sulfoxide)ruthenium(II) complexes $(\text{RuX}_2(\text{DMSO})_4)_2$; X = Cl, Br): synthesis, structure, and antitumor activity. *Inorg. Chem.* **1988**, *27*, 4099–4106. (b) Scholz, M. S.; Bull, J. N.; Carrascosa, E.; Adamson, B. D.; Kosgei, G. K.; Rack, J. J.; Bieske, E. J. Linkage Photoisomerization of an Isolated Ruthenium Sulfoxide Complex: Sequential versus Concerted Rearrangement. *Inorg. Chem.* **2018**, *57*, 5701–5706. (c) Rack, J. J. Electron transfer triggered sulfoxide isomerization in ruthenium and osmium complexes. *Coord. Chem. Rev.* **2009**, *253*, 78–85.

(36) Kost, T.; Sigalov, M.; Goldberg, I.; Ben-Asuly, A.; Lemcoff, N. G. Latent sulfur chelated ruthenium catalysts: Steric acceleration effects on olefin metathesis. *J. Organomet. Chem.* **2008**, *693*, 2200–2203.

(37) (a) Debieux, J.-L.; Bochet, C. G. The all-photochemical synthesis of an OGP(10–14) precursor. *Chem. Sci.* **2012**, *3*, 405–406. (b) San Miguel, V.; Bochet, C. G.; del Campo, A. Wavelength-Selective Caged Surfaces: How Many Functional Levels Are Possible? *J. Am. Chem. Soc.* **2011**, *133*, 5380–5388. (c) Blanc, A.; Bochet, C. G. Isotope Effects in Photochemistry: Application to Chromatic Orthogonality. *Org. Lett.* **2007**, *9*, 2649–2651.

(38) (a) Lerch, M. M.; Hansen, M. J.; Velema, W. A.; Szymanski, W.; Feringa, B. L. Orthogonal photoswitching in a multifunctional molecular system. *Nat. Commun.* **2016**, *7*, 12054. (b) Hansen, M. J.; Velema, W. A.; Lerch, M. M.; Szymanski, W.; Feringa, B. L. Wavelength-selective cleavage of photoprotecting groups: strategies and applications in dynamic systems. *Chem. Soc. Rev.* **2015**, *44*, 3358–

3377. (c) Brieke, C.; Rohrbach, F.; Gottschalk, A.; Mayer, G.; Heckel, A. Light-Controlled Tools. *Angew. Chem., Int. Ed.* **2012**, *51*, 8446–8476.

(39) (a) Schmidt, B.; Nave, S. Synthesis of Dihydrofurans and Dihydropyrans with Unsaturated Side Chains Based on Ring Size-Selective Ring-Closing Metathesis. *Adv. Synth. Catal.* **2007**, *349*, 215–230. (b) Schmidt, B.; Nave, S. Control of ring size selectivity by substrate directable RCM. *Chem. Commun.* **2006**, 2489–2491.

(40) (a) Brook, M. A.; Balduzzi, S.; Mohamed, M.; Gottardo, C. The photolytic and hydrolytic lability of silyl (Si(SiMe₃)₃) ethers, an alcohol protecting group. *Tetrahedron* **1999**, *55*, 10027–10040. (b) Brook, M. A.; Gottardo, C.; Balduzzi, S.; Mohamed, M. The silyl (tris(trimethylsilyl)silyl) group: A fluoride resistant, photolabile alcohol protecting group. *Tetrahedron Lett.* **1997**, *38*, 6997–7000.

(41) Sutar, R. L.; Levin, E.; Butilkov, D.; Goldberg, I.; Reany, O.; Lemcoff, N. G. A Light-Activated Olefin Metathesis Catalyst Equipped with a Chromatic Orthogonal Self-Destruct Function. *Angew. Chem., Int. Ed.* **2016**, *55*, 764–767.

(42) (a) Eivgi, O.; Levin, E.; Lemcoff, N. G. Modulation of Photodeprotection by the Sunscreen Protocol. *Org. Lett.* **2015**, *17*, 740–743. (b) Eivgi, O.; Lemcoff, N. G. Sunscreen-Assisted Selective Photochemical Transformations. *Molecules* **2020**, *25*, 2125.

(43) (a) Pump, E.; Leitgeb, A.; Kozłowska, A.; Torvisco, A.; Falivene, L.; Cavallo, L.; Grela, K.; Slugovc, C. Variation of the Sterical Properties of the N-Heterocyclic Carbene Coligand in Thermally Triggerable Ruthenium-Based Olefin Metathesis Precatalysts/Initiators. *Organometallics* **2015**, *34*, 5383–5392. (b) Huang, J.; Stevens, E. D.; Nolan, S. P.; Petersen, J. L. Olefin Metathesis-Active Ruthenium Complexes Bearing a Nucleophilic Carbene Ligand. *J. Am. Chem. Soc.* **1999**, *121*, 2674–2678. (c) Credendino, R.; Poater, A.; Ragone, F.; Cavallo, L. A computational perspective of olefins metathesis catalyzed by N-heterocyclic carbene ruthenium (pre)catalysts. *Catal. Sci. Technol.* **2011**, *1*, 1287–1297. (d) Samojłowicz, C.; Bieniek, M.; Grela, K. Ruthenium-Based Olefin Metathesis Catalysts Bearing N-Heterocyclic Carbene Ligands. *Chem. Rev.* **2009**, *109*, 3708–3742. (e) Trnka, T. M.; Grubbs, R. H. The Development of L₂X₂Ru=CHR Olefin Metathesis Catalysts: An Organometallic Success Story. *Acc. Chem. Res.* **2001**, *34*, 18–29. (f) Scholl, M.; Ding, S.; Lee, C. W.; Grubbs, R. H. Synthesis and Activity of a New Generation of Ruthenium-Based Olefin Metathesis Catalysts Coordinated with 1,3-Dimesityl-4,5-dihydroimidazol-2-ylidene Ligands. *Org. Lett.* **1999**, *1*, 953–956.

(44) (a) Fürstner, A.; Ackermann, L.; Gabor, B.; Goddard, R.; Lehmann, C. W.; Mynott, R.; Stelzer, F.; Thiel, O. R. Comparative Investigation of Ruthenium-Based Metathesis Catalysts Bearing N-Heterocyclic Carbene (NHC) Ligands. *Chem. - Eur. J.* **2001**, *7*, 3236–3253. (b) Clavier, H.; Urbina-Blanco, C. A.; Nolan, S. P. Indenylidene Ruthenium Complex Bearing a Sterically Demanding NHC Ligand: An Efficient Catalyst for Olefin Metathesis at Room Temperature. *Organometallics* **2009**, *28*, 2848–2854.

(45) Stewart, I. C.; Douglas, C. J.; Grubbs, R. H. Increased Efficiency in Cross-Metathesis Reactions of Sterically Hindered Olefins. *Org. Lett.* **2008**, *10*, 441–444.

(46) Ivry, E.; Frenklah, A.; Ginzburg, Y.; Levin, E.; Goldberg, I.; Kozuch, S.; Lemcoff, N. G.; Tzur, E. Light- and Thermal-Activated Olefin Metathesis of Hindered Substrates. *Organometallics* **2018**, *37*, 176–181.

(47) Lavallo, V.; Canac, Y.; Präsang, C.; Donnadiu, B.; Bertrand, G. Stable Cyclic (Alkyl)(Amino)Carbenes as Rigid or Flexible, Bulky, Electron-Rich Ligands for Transition-Metal Catalysts: A Quaternary Carbon Atom Makes the Difference. *Angew. Chem., Int. Ed.* **2005**, *44*, 5705–5709.

(48) Anderson, D. R.; Lavallo, V.; O'Leary, D. J.; Bertrand, G.; Grubbs, R. H. Synthesis and Reactivity of Olefin Metathesis Catalysts Bearing Cyclic (Alkyl)(Amino)Carbenes. *Angew. Chem., Int. Ed.* **2007**, *46*, 7262–7265.

(49) Marx, V. M.; Sullivan, A. H.; Melaimi, M.; Virgil, S. C.; Keitz, B. K.; Weinberger, D. S.; Bertrand, G.; Grubbs, R. H. Cyclic Alkyl Amino Carbene (CAAC) Ruthenium Complexes as Remarkably Active Catalysts for Ethenolysis. *Angew. Chem., Int. Ed.* **2015**, *54*, 1919–1923.

(50) (a) Butilkov, D.; Frenklah, A.; Rozenberg, I.; Kozuch, S.; Lemcoff, N. G. Highly Selective Olefin Metathesis with CAAC-Containing Ruthenium Benzylidenes. *ACS Catal.* **2017**, *7*, 7634–7637. (b) Gawin, R.; Tracz, A.; Chwalba, M.; Kozakiewicz, A.; Trzaskowski, B.; Skowerski, K. Cyclic Alkyl Amino Ruthenium Complexes—Efficient Catalysts for Macrocyclization and Acrylonitrile Cross Metathesis. *ACS Catal.* **2017**, *7*, 5443–5449.

(51) (a) Nascimento, D. L.; Gawin, A.; Gawin, R.; Guńka, P. A.; Zachara, J.; Skowerski, K.; Fogg, D. E. Integrating Activity with Accessibility in Olefin Metathesis: An Unprecedentedly Reactive Ruthenium–Indenylidene Catalyst. *J. Am. Chem. Soc.* **2019**, *141*, 10626–10631. (b) Nascimento, D. L.; Fogg, D. E. Origin of the Breakthrough Productivity of Ruthenium–Cyclic Alkyl Amino Carbene Catalysts in Olefin Metathesis. *J. Am. Chem. Soc.* **2019**, *141*, 19236–19240. (c) Ton, S. J.; Fogg, D. E. The Impact of Oxygen on Leading and Emerging Ru–Carbene Catalysts for Olefin Metathesis: An Unanticipated Correlation Between Robustness and Metathesis Activity. *ACS Catal.* **2019**, *9*, 11329–11334.

(52) Rozenberg, I.; Eivgi, O.; Frenklah, A.; Butilkov, D.; Kozuch, S.; Goldberg, I.; Lemcoff, N. G. Synthesis and Catalytic Properties of Sulfur-Chelated Ruthenium Benzylidenes Bearing a Cyclic (Alkyl)-(amino)carbene Ligand. *ACS Catal.* **2018**, *8*, 8182–8191.

(53) (a) Tzur, E.; Szadkowska, A.; Ben-Asuly, A.; Makal, A.; Goldberg, I.; Woźniak, K.; Grela, K.; Lemcoff, N. G. Studies on Electronic Effects in O-, N- and S-Chelated Ruthenium Olefin-Metathesis Catalysts. *Chem. - Eur. J.* **2010**, *16*, 8726–8737. (b) Szadkowska, A.; Makal, A.; Woźniak, K.; Kadyrov, R.; Grela, K. Ruthenium Olefin Metathesis Initiators Bearing Chelating Sulfoxide Ligands. *Organometallics* **2009**, *28*, 2693–2700. (c) Żukowska, K.; Pączek, Ł.; Grela, K. Sulfoxide-Chelated Ruthenium Benzylidene Catalyst: a Synthetic Study on the Utility of Olefin Metathesis. *ChemCatChem* **2016**, *8*, 2817–2823.

(54) Segalovich-Gerendash, G.; Rozenberg, I.; Allassad, N.; Nechmad, N. B.; Goldberg, I.; Kozuch, S.; Lemcoff, N. G. Imposing latency in ruthenium sulfoxide-chelated benzylidenes: Expanding opportunities for thermal and photoactivation in olefin metathesis. *ACS Catal.* **2020**, *10*, 4827–4834.

(55) (a) Guidone, S.; Songis, O.; Nagra, F.; Cazin, C. S. J. Conducting Olefin Metathesis Reactions in Air: Breaking the Paradigm. *ACS Catal.* **2015**, *5* (5), 2697–2701. (b) Bantreil, X.; Poater, A.; Urbina-Blanco, C. A.; Bidal, Y. D.; Falivene, L.; Randall, R. A. M.; Cavallo, L.; Slawin, A. M. Z.; Cazin, C. S. J. Synthesis and Reactivity of Ruthenium Phosphite Indenylidene Complexes. *Organometallics* **2012**, *31*, 7415–7426.

(56) Schmid, T. E.; Bantreil, X.; Citadelle, C. A.; Slawin, A. M. Z.; Cazin, C. S. J. Phosphites as ligands in ruthenium-benzylidene catalysts for olefin metathesis. *Chem. Commun.* **2011**, 47, 7060–7062.

(57) Lexer, C.; Burtscher, D.; Perner, B.; Tzur, E.; Lemcoff, N. G.; Slugovc, C. Olefin metathesis catalyst bearing a chelating phosphine ligand. *J. Organomet. Chem.* **2011**, *696*, 2466–2470.

(58) Although the reported yields in ref 4 are relatively low, an updated procedure with high yields was developed (Eivgi, O.; Vaisman, A.; Lemcoff, N. G., unpublished results).

(59) *polySpectra website*. <https://polyspectra.com/> (accessed 2020-09-06).

(60) (a) Phatake, R. S.; Masarwa, A.; Lemcoff, N. G.; Reany, O. Tuning thermal properties of cross-linked DCPD polymers by functionalization, initiator type and curing methods. *Polym. Chem.* **2020**, *11*, 1742–1751. (b) Vidavsky, Y.; Navon, Y.; Ginzburg, Y.; Gottlieb, M.; Lemcoff, N. G. Thermal properties of ruthenium alkylidene-polymerized dicyclopentadiene. *Beilstein J. Org. Chem.* **2015**, *11*, 1469–1474. (c) Saha, S.; Ginzburg, Y.; Rozenberg, I.; Iliashvsky, O.; Ben-Asuly, A.; Gabriel Lemcoff, N. Cross-linked ROMP polymers based on odourless dicyclopentadiene derivatives. *Polym. Chem.* **2016**, *7*, 3071–3075.

(61) Robertson, I. D.; Dean, L. M.; Rudebusch, G. E.; Sottos, N. R.; White, S. R.; Moore, J. S. Alkyl Phosphite Inhibitors for Frontal Ring-Opening Metathesis Polymerization Greatly Increase Pot Life. *ACS Macro Lett.* **2017**, *6*, 609–612.